Transcription Factor MYB26 Is Key to Spatial Specificity in Anther Secondary Thickening Formation[1][CC-BY]

Caiyun Yang,[a] Jie Song,[a,2] Alison C. Ferguson,[a] Doris Klisch,[a] Kim Simpson,[a] Rui Mo,[a] Benjamin Taylor,[a] Nobutaka Mitsuda,[b] and Zoe A. Wilson[a,3]

[a]School of Biosciences, University of Nottingham, Sutton Bonington Campus, Loughborough, Leicestershire LE12 5RD, United Kingdom

[b]Bioproduction Research Institute, National Institute of Advanced Industrial Science and Technology (AIST). Üentral 6, Higashi 1-1-1, Tsukuba, Ibaraki 305-8566, Japan

ORCID IDs: 0000-0002-0521-4230 (C.Y.); 0000-0003-1635-9598 (J.S.); 0000-0002-3532-1782 (A.C.F.); 0000-0002-5772-2261 (D.K.); 0000-0002-7741-6018 (R.M.); 0000-0001-5689-3678 (N.M.); 0000-0003-0948-8770 (Z.A.W.).

Successful fertilization relies on the production and effective release of viable pollen. Failure of anther opening (dehiscence), results in male sterility, although the pollen may be fully functional. MYB26 regulates the formation of secondary thickening in the anther endothecium, which is critical for anther dehiscence and fertility. Here, we show that although the *MYB26* transcript shows expression in multiple floral organs, the MYB26 protein is localized specifically to the anther endothecium nuclei and that it directly regulates two *NAC* domain genes, *NST1* and *NST2*, which are critical for the induction of secondary thickening biosynthesis genes. However, there is a complex relationship of regulation between these genes and MYB26. Using DEX-inducible MYB26 lines and overexpression in the various mutant backgrounds, we have shown that MYB26 up-regulates both *NST1* and *NST2* expression. Surprisingly normal thickening and fertility rescue does not occur in the absence of MYB26, even with constitutively induced *NST1* and *NST2*, suggesting an additional essential role for MYB26 in this regulation. Combined overexpression of *NST1* and *NST2* in *myb26* facilitates limited ectopic thickening in the anther epidermis, but not in the endothecium, and thus fails to rescue dehiscence. Therefore, by a series of regulatory controls through MYB26, NST1, NST2, secondary thickening is formed specifically within the endothecium; this specificity is essential for anther opening.

Fertilization is important for seed production; a number of factors are required for successful fertilization, such as the production of viable pollen and then its efficient release at the optimal time to allow for pollination. Failure of pollen release results in male sterility even if the pollen itself is fully functional. Pollen is formed within anthers, a specialized structure that is supported on a filament, which provides vascular connections to the developing anther. The filament also enables the anther to extend and protrude away from the petals to facilitate effective pollen dispersal. The anther is comprised of four cell layers, which encase the microspores as they develop into mature pollen grains: the tapetum, middle cell layer, endothecium, and the outer epidermal layer. Defects in these cell layers, particularly the tapetum, frequently result in a failure of pollen development, with the degeneration of the pollen, empty anther locules, and male sterility (Scott et al., 2004; Ma, 2005; Ariizumi and Toriyama, 2011). The endothecium, however, plays a principal role in anther dehiscence by providing the force required for opening due to localized secondary thickening and anther dehydration.

After microspore release, the endothecium layer starts to undergo selective expansion followed by secondary thickening, and specific epidermal cells differentiate to form the stomium region. This region subsequently defines the position of anther opening and does not develop the secondary thickening seen in the endothecium and connective tissues. Dehiscence is a two-phase process involving initial enzymatic degradation of the septum separating the two locules, followed by retraction of the locules resulting in a split at the stomium (Wilson et al., 2011). By a combination of molecular genetic analysis and mathematical modeling, we have shown that the mechanical control of opening is mediated by the bilayer structure of the mature anther wall (Nelson et al., 2012). This is comprised of an outer epidermal cell layer, whose turgor pressure is related to its hydration, and the endothecial layer, whose walls contain helical secondary thickening that resist stretching and bending. This model predicts that epidermal dehydration, in association with the thickened

[1] This work was funded by the Biotechnology and Biological Science Research Council (BB/F021062/1 and BB/J001295/1); R.M. was supported by a PhD Scholarship from the China Scholarship Council.

[2] Current address: Department of Life Sciences, South Kensington Campus, Imperial College London, London SW7 2AZ, United Kingdom.

[3] Address correspondence to zoe.wilson@nottingham.ac.uk.

The author responsible for distribution of materials integral to the findings presented in this article in accordance with the policy described in the Instructions for Authors (www.plantphysiol.org) is: Zoe A. Wilson (zoe.wilson@nottingham.ac.uk).

Z.A.W. designed the research; C.Y., J.S., A.C.F., D.K., K.S., R.M., and B.T. performed the research; C.Y., J.S., A.C.F., R.M., B.T., Z.A.W. analyzed the data; N.M. generated the NST1/2:GUS lines; Z.A.W., C.Y., J.S., and A.C.F. wrote the manuscript.

www.plantphysiol.org/cgi/doi/10.1104/pp.17.00719

endothecial layer, creates forces in the anther wall, causing it to bend outwards, which results in splitting of the stomium, locule retraction, anther opening, and pollen release (Nelson et al., 2012). The requirement for endothecium thickening for dehiscence has been demonstrated genetically by mutants of *MYB26/MALE STERILE35* (Dawson et al., 1993; Steiner-Lange et al., 2003) and *NAC SECONDARY WALL THICKENING PROMOTING FACTOR1* (*NST1*) and *NST2* (Mitsuda et al., 2005). Both the *myb26* and *nst1nst2* mutants produce viable pollen but lack endothecium secondary thickening and are male sterile because the pollen is not released.

We previously showed that the *MYB26* gene is able to induce ectopic secondary thickening when expressed under the control of the *CaMV35S* promoter (Yang et al., 2007). Similar phenotypes to those seen with *MYB26* are also generated by overexpression of the *NST1* and *NST2* genes (Mitsuda et al., 2005). Cecchetti et al. (2013) demonstrated that the timing of anther dehiscence was negatively regulated by auxin inhibiting *MYB26* expression and thus endothecium lignification, but also stomium opening via the control of jasmonic acid (JA) biosynthesis. It has recently been shown that an auxin maxima is formed due to transport of auxin from the tapetum into the middle cell layer, and this is important for the regulation of pollen development and dehiscence (Cecchetti et al., 2017).

NST1 and *NST2* belong to the large NAC-domain family, which is made up of plant-specific transcription factors associated with a variety of developmental processes (Olsen et al., 2005). A subgroup of these has been identified as master regulators of secondary thickening. These appear to function redundantly in groups exhibiting differential expression throughout the plant. *NST3/SECONDARY WALL ASSOCIATED NAC DOMAIN PROTEIN1* (*SND1*; *At1g32770*) are specifically expressed in fibers (Zhong et al., 2006; Mitsuda et al., 2007; Mitsuda and Ohme-Takagi, 2008), while *VASCULAR RELATED NAC-DOMAIN1–7* (*VND1–VND7*) are expressed in vessels with VND6 and VND7 important for the formation of proto and metaxylem, and VND1–5 for parenchyma cells (Kubo et al., 2005; Yamaguchi et al., 2008; Zhong et al., 2008; Zhou et al., 2014). *NST1* and *NST2* act redundantly to facilitate secondary thickening in the anther (Mitsuda et al., 2005). Previous work has shown that *NST2* is expressed predominantly in the anther with some expression in the interfascicular fibers and xylary fibers (Zhong and Ye, 2015), whereas *NST1* is expressed in the anther and other tissues where secondary thickening is observed, where it acts alongside *NST3/SND1* to regulate secondary wall biosynthesis in these tissues (Mitsuda et al., 2005). The double mutant *nst1snd1* only has limited thickening within these tissues suggesting that *NST2* plays a minor role in the regulation of secondary wall biosynthesis in fibers (Zhong and Ye, 2015).

The anther endothecium thickening forms as striated bands that resemble tracheary elements and are formed of lignocellulose, as indicated by phloroglucinol and ethidium acridine-orange staining (Dawson et al., 1999; Yang et al., 2007). The composition of the thickening appears to be critical for dehiscence, since the triple *ccc* mutant, which is defective for *cinnamoyl CoA reductase1*, *cinnamyl alcohol dehydrogenase c* and *cinnamyl alcohol dehydrogenase d*, has hypolignified stems and accumulates higher amounts of flavonol glycosides, sinapoyl malate. and feruloyl malate, has abnormal endothecium thickening, and is male sterile (Thévenin et al., 2011).

Previous studies have demonstrated the roles that the NAC domain genes play in regulating secondary thickening biosynthesis genes; however, little is known regarding the relationship between the NAC domain genes and the upstream transcription factors that regulate the tissue specificity of secondary thickening formation. Here, we have conducted a molecular genetic analysis of the interactions between the *MYB26* and *NST1/NST2* genes, which has shown that MYB26 is an initial switch required for subsequent secondary thickening formation in the anther, acting directly via regulating *NST1* and *NST2*. Using a functional inducible translational fusion, we have shown that the MYB26 protein is nuclear localized specifically within the anther endothecium, despite the transcript being detected in multiple cell layers in the anther. We have also shown that expression of NST1/NST2 cannot rescue dehiscence and fertility in the *myb26* mutant, thus demonstrating that the downstream *NST1/NST2* factors are insufficient for secondary thickening and that expression of *MYB26* and presumably the equivalent regulator in the vegetative tissues is essential for correctly localized secondary thickening formation. This series of controls ensures the specificity of location of secondary thickening, which is essential for anther dehiscence.

RESULTS

Dexamethasone-Inducible Expression of MYB26 Rescues Fertility in the *myb26* Mutant

A translational MYB26 fusion protein was constructed (*MYB26pro:MYB26-GR-YFP*) under the control of the native *MYB26* promoter, with the *MYB26* genomic sequence fused to the glucocorticoid receptor (GR) ligand-binding domain and *YFP* reporter gene; thus, the translated protein was localized in the cytoplasm and inactive until treated with dexamethasone (DEX), allowing it to become nuclear localized. The construct was transformed into heterozygous *myb26-MYB26* mutant plants, and the T1 generation was screened by Basta and PCR for the transgene. Confirmed transgenic plants were genotyped to identify *myb26* homozygous plants; these mutants carrying the MYB26-GR-YFP transgene were male sterile as expected (Fig. 1, A, C, and F), due to a failure of dehiscence because of a lack of secondary thickening in the endothecium, as seen in the *myb26* mutant (Fig. 1I). However, a single spray of 25 μM DEX solution on the

young flower buds was able to produce flowers with normal dehiscent anthers and rescued fertility (Fig. 1, B, D, G, and J).

The response of transgenic *myb26* mutant plants to the DEX was dependent on the stage of anther development during the treatment. Old unopened flower buds containing postpollen mitosis I stage anthers were not affected, and these formed short siliques without seeds. However in younger buds, prior to pollen mitosis I stage, that developed in the 4 to 7 d after the DEX treatment, full fertility was restored with anther dehiscence occurring normally and silique elongation as seen in wild type (Fig. 1D). Pollen development stage was confirmed using DAPI staining of the pollen, and this corresponded to when endothecium expansion and deposition of secondary thickening normally occurred (Sanders et al., 1999). The effect of a single DEX treatment lasted approximately 7 d; after this point, the plants reverted to sterility, unless the DEX treatment was repeated. The flowers from lines carrying the transgene appeared normal, with no ectopic thickening or abnormalities in the DEX-treated inducible lines regardless of whether the transgene was in the mutant or wild-type background (Fig. 1, E–G). Fertility was not affected in the wild-type transgenic lines by DEX treatment. The lignification of the endothecium in the complemented *myb26* mutant buds was variable, with some anthers forming a fully developed endothecial layer while others showed only a partially lignified endothecium layer (Fig. 1J). This did not appear to correspond to bud age and was possibly due to the uneven distribution of the DEX and nuclear-localized MYB26 within the anthers.

MYB26 Protein Is Specifically Localized to the Anther Endothecium

The *myb26* mutant lines carrying the functional MYB26-GR-YFP fusion protein were analyzed for localization of the MYB26-YFP protein. After DEX treatment the MYB26-YFP protein was observed in the nuclei of endothecium cells during the pollen mitosis I stage (Fig. 2, A and B). Prior to this, during pollen mother cell meiosis and microspore release and after pollen mitosis II, no MYB26-YFP expression was seen. No MYB26-YFP expression was seen in other tissues in the flowers or vegetative tissues despite detection of GUS expression using the same length promoter in a transcriptional fusion (*MYB26pro:GUS*) in the nectaries, style, filaments, and anthers (Fig. 2C).

MYB26 expression was determined by time course quantitative reverse transcription (qRT)-PCR analysis in buds from the inducible line; expression showed an initial fluctuation immediately post-DEX treatment (and thus nuclear localization of the MYB26 protein); however, approximately 3 h post-DEX treatment reduced *MYB26* expression was seen, which was subsequently maintained throughout the analysis (72 h; Fig. 2D). This suggests that the functional MYB26 protein may directly or indirectly inhibit its own (*MYB26*) expression.

*MYB*26 Can Induce Expression of *NST1* and *NST2*, But Cannot Rescue Secondary Thickening in the *nst1nst2* Mutant Background

Previous work suggested that *MYB26* may act upstream of the two NAC domain genes *NST1* and *NST2*, with a reduction of the expression of both these genes in the *myb26* mutant, and up-regulation in *MYB26* overexpression line (Yang et al., 2007); however, the genetic relationship between these genes has not been fully established. The ability of MYB26 to induce *NST1* and *NST2* expression and regulate secondary thickening in the absence of *NST1NST2* expression was therefore investigated. Expression of *NST1* and *NST2* was analyzed in lines overexpressing *MYB26* (regulated by the CaMV35S promoter), and in our DEX-inducible MYB26 line (*MYB26pro:MYB26-GR-YFP* in the *myb26* mutant background). Increased expression of *NST1pro:GUS* was seen in the lines overexpressing *MYB26* (*35Spro:MYB26)* with intense *NST1pro:GUS* staining visible, particularly in the peduncle, sepals, and anthers (Fig. 3, B and C). Expression of *NST1* and *NST2* was analyzed by qRT-PCR over a 72 h period after MYB26 induction by DEX treatment; induction of *NST1* and *NST2* occurring approximately 4 to 6 h post-DEX treatment (Fig. 3, D and E). These data suggest that *NST1* and *NST2* are induced by and act downstream of MYB26. To confirm this and to check whether overexpression of *MYB26* was able to rescue fertility in the double *nst1nst2* mutant, the *nst1nst1NST2nst2* heterozygous mutant was transformed with the *35Spro:MYB26* construct (see "Materials and Methods"). Transgenic lines were selected on hygromycin plates and PCR screened for presence of the *MYB26* transgene and segregation of the *nst2* mutation. T1 and T2 transgenic lines were analyzed for male fertility, anther development, and secondary thickening in anther and vegetative tissues. qRT-PCR was also conducted to establish the levels of *MYB26* and *NST1/2* gene expression.

NST1 and *NST2* have been previously shown to act redundantly, with male sterility in the double mutant but normal fertility and vegetative growth seen if one functional *NST1* or *NST2* copy is present (Mitsuda et al., 2005). We also observed that the *nst1nst2* double mutant was male sterile as previously reported (Mitsuda et al., 2005), with viable pollen but indehiscent anthers due to a lack of secondary thickening in the anther endothecium (Fig. 4, B and F). Secondary thickening was still present in the inflorescence stem and other tissues in the *nst1nst2* mutant, if slightly reduced compared to wild type (Fig. 4, I and J), presumably due to the normal expression of *NST3/SND1*, which acts redundantly with *NST1* in the stem (Mitsuda et al., 2007). The *nst1nst2* double mutant tended to be bushier than the wild type (Fig. 4, A and B), probably due to the lack of *NST1* and *NST2* expression throughout the plant, as well as the reduced levels of

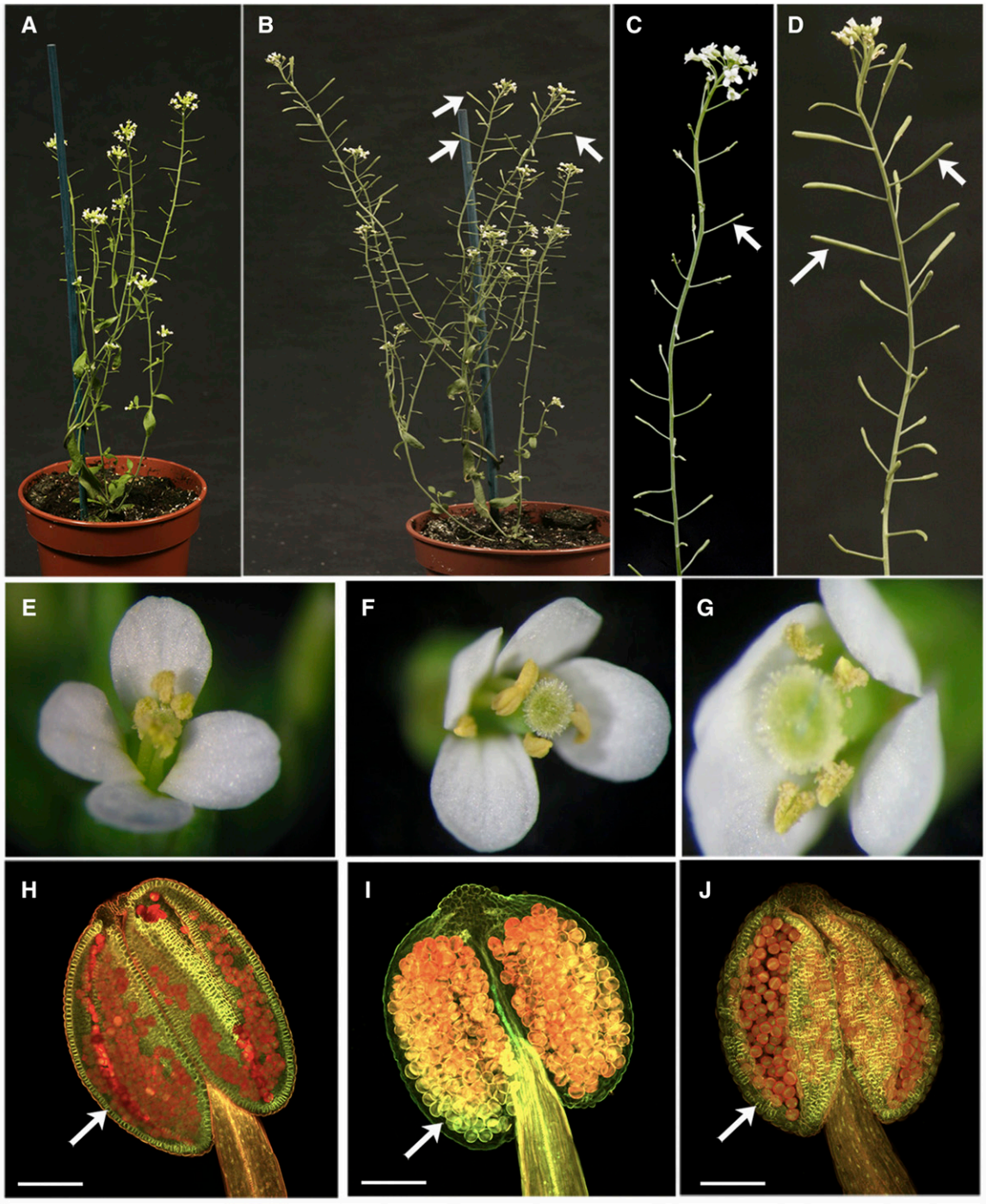

Figure 1. Rescue of fertility by DEX induction of MYB26. A, *myb26* mutant carrying the *MYB26pro:MYB26-GR-YFP* transgene line before DEX treatment showing short, sterile siliques due to a lack of self-fertilization as a result of a failure of anther dehiscence. B, *myb26* mutant carrying the *MYB26pro:MYB26-GR-YFP* transgene line after DEX treatment, showing rescued fertility and elongated, filled siliques on the upper region of the inflorescences (arrows); below the rescued fertile siliques were male sterile short, seedless siliques which developed before the DEX treatment. C, Close-up of the inflorescence from the transgene line before DEX treatment, showing short siliques (arrow), which do not contain seeds. D, Close-up of the inflorescence from the transgene line showing rescue of fertility and elongated, filled siliques (arrows) after DEX treatment. E, Wild-type flower showing anther dehiscence and pollen release. F, Flower from the *myb26* mutant carrying the *MYB26pro:MYB26-GR-YFP* transgene before DEX treatment, showing a lack of anther dehiscence and pollen release. G, Flower from the *myb26* mutant line carrying the *MYB26pro:MYB26-GR-YFP* transgene line after DEX treatment, showing rescue of anther dehiscence. H to J, Confocal images of anthers after ethidium bromide/acridine orange staining for secondary thickening. H, Wild-type anther showing lignified

fertilization and seed set in the double mutant. *MYB26* expression levels varied in buds from the whole inflorescence, between individual *nst1nst2* lines. In some instances, *MYB26* expression was slightly increased in the *nst1nst2* double mutant (Fig. 4M); however the minor changes observed suggests that the absence of *NST1* and *NST2* did not have a significant regulatory role on *MYB26* expression.

As expected, ectopic expression of *MYB26* under control of the *CaMV35S* promoter was unable to complement the male sterile phenotype of the *nst1nst2* double mutant (Fig. 4C), indicating it acts upstream of *NST1NST2*. These lines failed to produce endothecium secondary thickening (Fig. 4G) and therefore did not undergo anther dehiscence and pollen release. The heterozygous mutant *nst1nst1NST2nst2* carrying *35Spro:MYB26* was fertile due to the *NST2* expression alongside the *MYB26* expression but showed enhanced secondary thickening (Fig. 4, D and H). In this line, the expression of *NST2* was enhanced compared to wild type, presumably as a consequence of induction by the high levels of *MYB26* (Fig. 4M). This heightened expression of *NST2* therefore resulted in the increased anther secondary thickening observed in these lines (Fig. 4H). However, enhanced thickening in the anther was observed only in the endothecium, allowing normal anther dehiscence and fertility. No ectopic expression was seen in the other anther cell layers, suggesting that strong spatial regulation limiting secondary thickening deposition occurs in the anther and that NST2 is principally acting in the endothecium. Previously, when *MYB26* was overexpressed in the wild-type background, which is expressing both *NST1* and *NST2*, ectopic epidermal thickening was seen alongside increased endothecium thickening (Yang et al., 2007). This suggests that MYB26 acts with NST1/NST2, and that NST2 and MYB26 are principally acting in the endothecium, while NST1 is present in both cell layers. Therefore, the expression of NST1 in both endothecium and epidermal tissue allowing for the ectopic epidermal thickening when NST1 is up-regulated in this cell layer by constitutive MYB26 expression (*CaMV35S* promoter). The growth pattern of the *35Spro:MYB26* in the *nst1nst1NST2nst2* background appeared as wild type and did not show the bushiness seen in the *nst1nst2* mutant. This is likely to be a consequence of redundancy between *NST1* and *NST2* (Mitsuda et al., 2005) and the expression of *NST2*, which has been recently reported in stem tissues (Zhong and Ye, 2015), and rescue of sterility. The level of *MYB26* overexpression was also strongly increased in the presence of functional *NST2* (Fig. 4M), suggesting that *NST2* may also up-regulate or stabilize *MYB26* expression.

NST1 and *NST2* have been shown to act redundantly with *NST3/SND1*, which is expressed in the inflorescence stems, in the regulation of secondary wall thickenings in interfasicular fibers and secondary xylem (Mitsuda et al., 2007; Zhong and Ye, 2015). *NST3* expression was therefore also analyzed by qRT-PCR in buds from the *MYB26*-overexpressing lines. No significant native expression of *NST3* was seen in the floral tissues, although a slight increase in *NST3* was observed in the *nst1nst2* mutant samples (Fig. 4M). This may reflect a compensatory increase in *NST3* expression in the peduncle due to the absence of *NST1*. Although *NST3* is still expressed in the *nst1nst2* double mutant, the lack of significant ectopic thickening when *35Spro:MYB26* was expressed in the absence of *NST1* or *NST2* suggests that *MYB26* is principally acting via *NST1* and *NST2*, rather than *NST3*. Nevertheless, *NST3* expression was greatly increased in the *nst1nst1NST2nst2* line and by high levels of *MYB26* in the *NST2nst2* background (Fig. 4M); this increase was not seen in the *nst1nst2* lines overexpressing MYB26, suggesting that this up-regulation may be mediated by NST2 (and also potentially NST1), in combination with MYB26. Ectopic lignification of the stem tissues (Fig. 4L) and also other tissues, e.g. sepals and petals, was seen in the *nst1nst1NST2nst2* lines carrying the *35Spro:MYB26* gene, which may be due to the *MYB26* expression in the presence of *NST2* or increased *NST3* expression in the stem tissues, as this lignification was not seen in the double *nst1nst2* mutant lines overexpressing *MYB26*. qRT-PCR was also used to determine the effect of *MYB26* and *NST1NST2* on the expression of key genes linked to secondary thickening deposition. In the *nst1nst2* mutant inflorescences, there was a significant down-regulation of *IRREGULAR XYLEM1* (*IRX1*), *IRX3*, *IRX8*, and *IRX12*. Expression of *NST2* in *nst1nst1NST2nst2* rescued *IRX3* and *IRX12* expression, suggesting that *NST2* directly or indirectly regulates these genes (Fig. 4N), while presence of *NST2* and overexpression of MYB26 led to rescue of *IRX1* and *IRX8*, suggesting that these genes may also require the presence of *MYB26* or are primarily regulated by *NST2* and require increased *NST2* expression to reach normal levels. *IRX1/Ces8* and *IRX3/Ces7* have been shown to be coordinately expressed alongside *IRX5* and to interact to form the cellulose synthase complex (Taylor et al., 2003), whereas IRX8/Galacturonosyltransferase 12 (GAUT12) and IRX12/LACCASE are involved in xylan (Persson et al., 2005; Caffall et al., 2009) and lignin biosynthesis (Zhao et al., 2013), respectively. Other genes (*IRX4*, *IRX10*) associated with secondary thickening showed a slight reduction of expression in *nst1nst2* mutant and MYB26 overexpression in this double mutant background. *IRX4* expression was increased with the

Figure 1. (*Continued.*)
endothecium layer (arrow). I, *myb26* mutant carrying the *MYB26pro::MYB26-YFP-GR* transgene before DEX treatment, which lacks endothecium secondary thickening (arrow). J, *myb26 MYB26pro:MYB26-GR-YFP* transgene line showing restoration of endothecium thickening after DEX treatment (arrow). Scale bars: 100 μm.

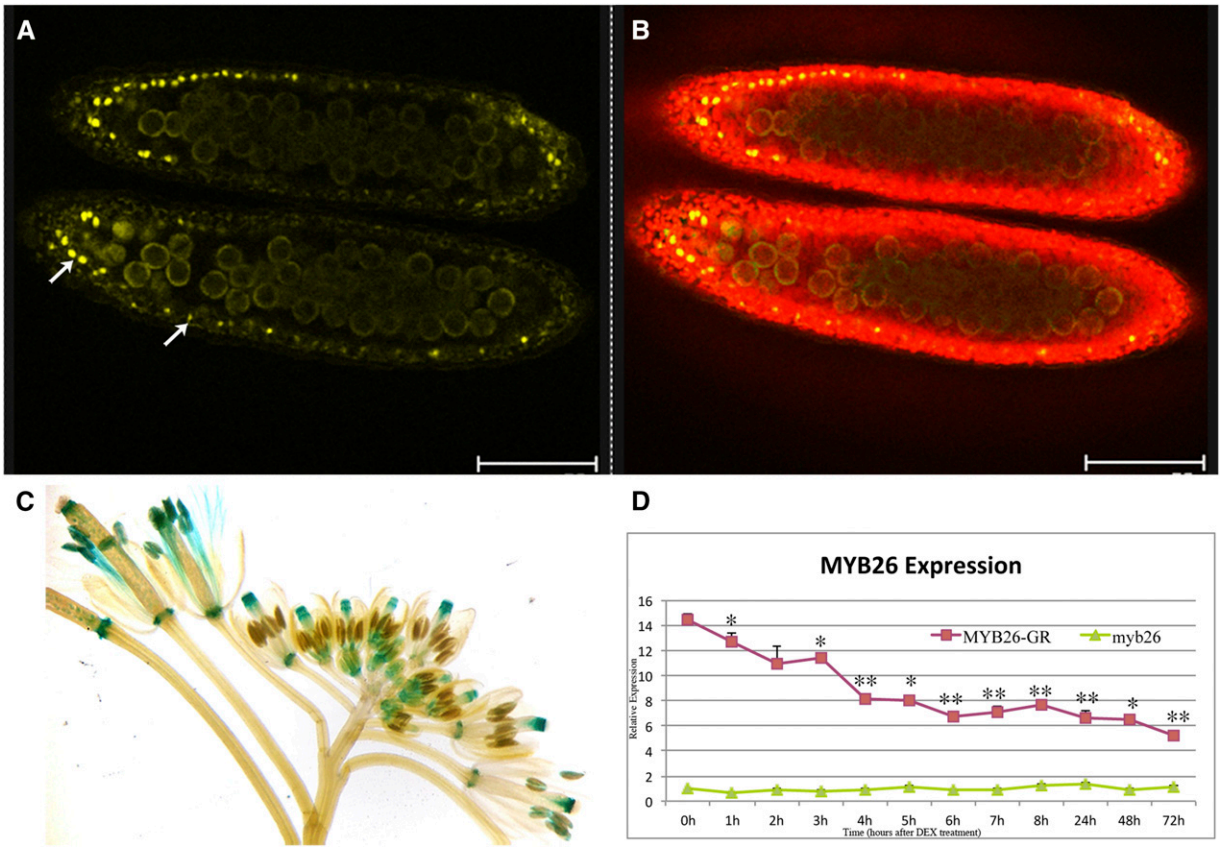

Figure 2. Localization of MYB26 after DEX-induced expression. A and B, Confocal imaging of expression of the functional *MYB26pro:MYB26-YFP* fusion protein in anthers; expression is only seen in the nuclei of the anther endothecium cells during pollen mitosis I. A, MYB26-YFP fusion protein localized in endothecium nuclei (arrows; excitation 514 nm). B, Overlay of anther chlorophyll autofluorescence (excitation 488 nm) and MYB26-YFP fusion protein. Scale bar represents 75 μm. C, *MYB26Pro:GUS* expression is seen in many floral tissues, including nectaries, style, filaments, and anthers. D, Time course of *MYB26* expression by qRT-PCR in *myb26* mutant buds and *myb26* mutant carrying the *MYB26pro:MYB26-GR-YFP* transgene after DEX treatment. Expression levels of the transgene fluctuated slightly but were reduced 1 h post-DEX treatment and strongly reduced by 4 h post-DEX treatment with all samples being at least $P < 0.05$ after 3 h compared to 0 h control (*t* test statistical analysis; $*P \leq 0.05$; $**P \leq 0.01$).

presence of *NST2* and overexpression of *MYB26* in the *nst1nst1NST2nst2* background, suggesting that the presence of *NST2* and *MYB26* is important for *IRX4* expression (Fig. 4N). While FRA8 showed a slight increase in expression in the presence of *NST2* (Fig. 4, M and N). This agrees with the observed development of endothecium secondary thickening and rescue of fertility in the *35Spro:MYB26 nst1nst1NST2nst2* lines, suggesting that *NST2* and *NST1* are acting downstream of MYB26 to regulate the biosynthesis of secondary thickening, including cellulose, hemicelluloses, and lignin biosynthesis.

Chromatin Immunoprecipitation (ChIP)-PCR Enrichment Supports MYB26 as Directly Regulating *NST1* and *NST2*

ChIP-PCR analysis was conducted to establish if the interaction between MYB26 and *NST1/2* was via direct binding using a number of upstream regions of the *NST1* and *NST2* genes (Fig. 5, A and B) and a peptide-derived anti-MYB26 antibody with chromatin isolated from *35Spro:MYB26-GFP* buds (Fig. 5D). An independent experiment using an anti-GFP antibody with buds collected from the *MYB26pro:MYB26-GR-YFP* line, which had been DEX-induced with the noninduced line as a control (mock), was also conducted (Fig. 5, C and F). MYB26-YFP within the nucleus of the endothecium was detected in the DEX-induced *MYB26pro:MYB26-GR-YFP* line (Fig. 5E). In both experiments, enrichment was seen in selected regions of the *NST1* and *NST2* promoter compared to negative controls of negative promoter fragments or nonspecific antibodies (IpG; Fig. 5, C, D and F). EMSA was subsequently conducted to further confirm this result; however, no retardation was observed (data not shown). ChIP therefore indicates that direct binding is occurring between MYB26 and *NST1* and -2, but the lack of gel retardation implies that another factor/modification is needed for this

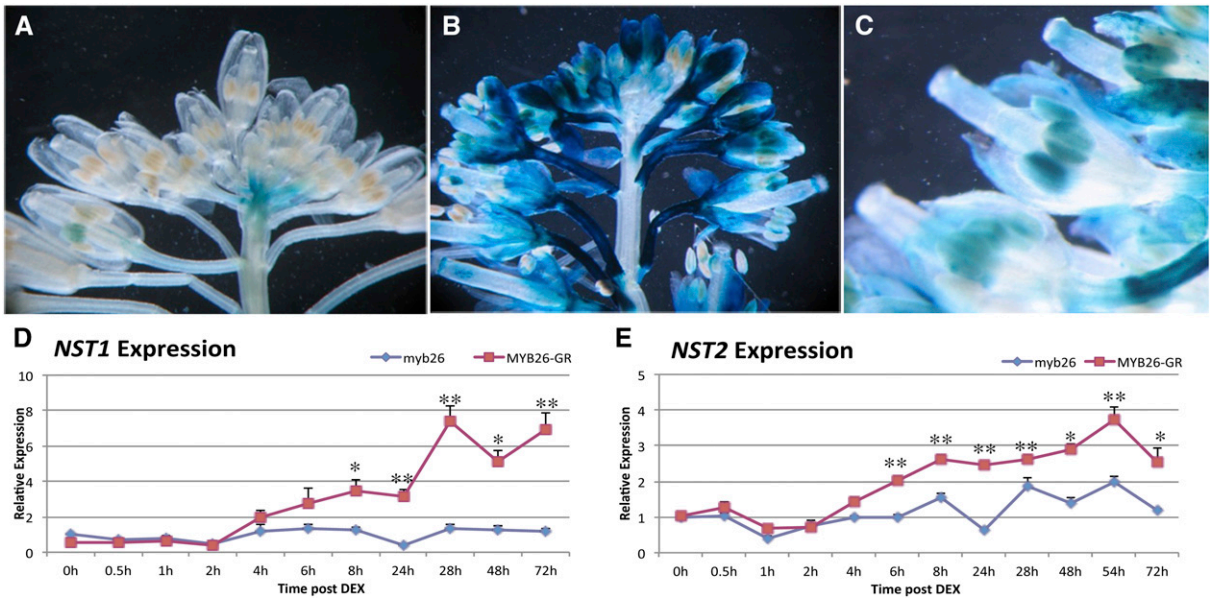

Figure 3. Induction of *NST1* and *NST2* expression by MYB26. A, *NST1Pro:GUS* expression in wild type and (B) increased *NST1pro:GUS* expression in *MYB26* overexpression line, particularly in the peduncle, sepals. and anthers. C, Increased magnification of *NST1pro:GUS* expression in *MYB26* overexpression line showing expression in anthers. D and E, Time course analysis of expression of *NST1* and *NST2* by qRT-PCR after DEX activation of MYB26 in the transgenic (*MYB26pro:MYB26-GR-YFP*) *myb26* mutant line and in the *myb26* mutant control lacking the transgene. D, Induction of *NST1* occurred 4 to 6 h after DEX treatment. E, Induction of *NST2* was seen 4 to 6 h after DEX treatment. Error bars represent SD (*t* test statistical analysis compared to 0 h in each line; $*P \leq 0.05$; $**P \leq 0.01$).

regulation or that the conditions for in vitro binding were not suitable for complex formation.

Overexpression of *NST1* and *NST2* Cannot Complement the *myb26* Mutation

Previously it has been shown that individually the *MYB26*, *NST1*, and *NST2* gene under control of the *CaMV35S* promoter induced ectopic secondary thickening (Mitsuda et al., 2005; Yang et al., 2007). Given that the *NST1* and *NST2* genes are responsible for induction of secondary thickening biosynthesis genes and appear to be downstream and regulated by MYB26, we tried to complement the *myb26* mutation by overexpression of *NST1* and *NST2* using the *CaMV35S* promoter. Secondary thickening in anthers was observed using a combined stain of ethidium bromide, which indicates lignified cells (red fluorescence) and acridine orange, which stains lignified walls with a drop in fluorescence for nonlignified walls (green fluorescence; Stockert et al., 1984; Yang et al., 2007; Thévenin et al., 2011). As previously reported, we observed that the *myb26* mutant failed to develop endothecium thickening (Fig. 6, C and D). As expected in the wild-type background, both the *35Spro:NST1* and *35Spro:NST2* lines showed increased secondary thickening in the flowers and leaves. In the wild-type anthers when *NST2* was overexpressed, this was limited to the endothecium cell layer (Fig. 6, G and K), whereas when *NST1* was expressed, using the same *CaMV35S* promoter, thickening was seen in the epidermis as well and in the endothecium (Fig. 6, E and I). However, when either *NST1* or *NST2* was overexpressed in the *myb26* mutant background, the levels of secondary thickening in the anthers were not significantly increased (Fig. 6, F, J, H, and L), with no significant secondary thickening forming except limited secondary thickening in a very few isolated epidermal cells. This analysis was initially conducted using *myb26* SALK_112372 insertional mutant but was subsequently repeated using the *ms35* x-ray mutant *ms35gl*, in case gene silencing of the transgene was occurring as both constructs contained the *CaMV35S* promoter. Similar results were seen with these lines: increased secondary thickening in the endothecium (*NST1* and *NST2*) and epidermis (*NST1*) in the heterozygous *ms35MS35* and a lack of ectopic thickening without *MYB26* expression except for the occasional isolated epidermal cell (Supplemental Fig. S1). This suggests that *NST1* or *NST2* singularly in the absence of MYB26 are not able to induce secondary thickening and that the presence of *MYB26* in the anther is required to initiate normal endothecium thickening; nevertheless, MYB26 is acting through *NST1/2*. This lack of complementation by *NST1/2* expression may be a reflection that *MYB26* is controlling the expression of an additional factor that is required for accumulation, or potentially activation, of the *NST1/2* transcripts; for example, this could be acting by the removal of a repressor that serves to limit the level of *NST1* and *NST2* transcript.

qRT-PCR indicated that the levels of *NST1* and *NST2* expression (*35Spro:NST1* or *35Spro:NST2*) were greatly

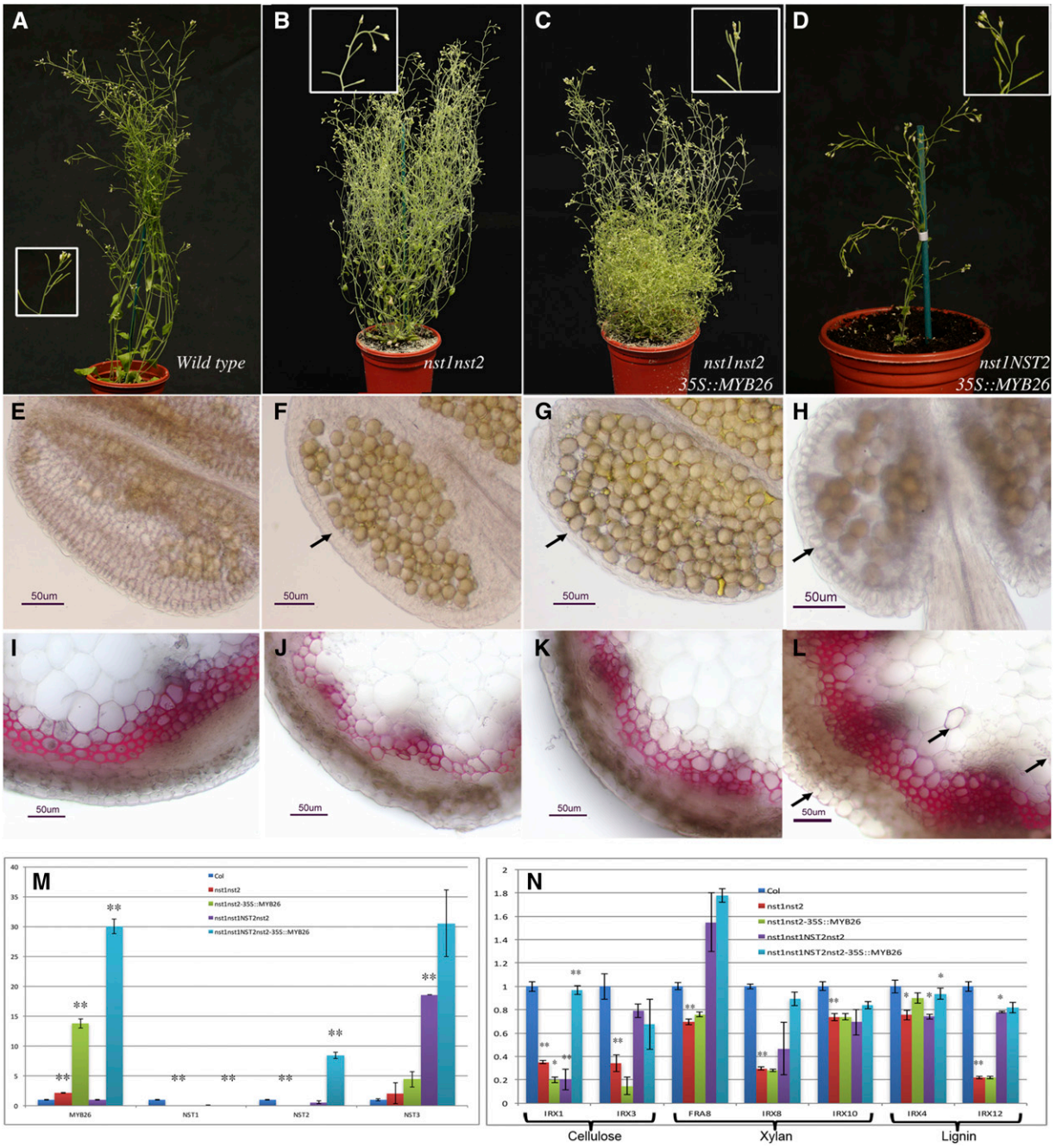

Figure 4. Ectopic expression of *MYB26* is unable to induce secondary thickening in the anther in the absence of *NST1* or *NST2* expression. A, Wild-type plant showing full fertility as evidenced by silique elongation and full seed set. B, *nst1nst2* double mutant showing sterility as indicated by a lack of silique elongation; plants also showed increased bushy growth. C, Expression of *35Spro:MYB26* in *nst1nst2* background does not rescue male fertility or bushy growth. D, Expression of *35Spro:MYB26* in *nst1nst1NST2nst2* background, which is heterozygous for and thus expressing *NST2*, is fertile, and growth resembles wild type. *NST2* acts redundantly with *NST1*, and the phenotypes of heterozygous lines are equivalent to wild type, with full fertility and normal growth habit (Mitsuda et al., 2005). Boxed regions show increased magnification of the same lines. E to L, Sections stained with phloroglucinol to detect lignin; scale bar represents 50 μm. E Wild-type anther showing secondary thickening in the endothecium. F The *nst1nst2* double mutant fails to develop endothecium secondary thickening (arrow). G, Endothecium secondary thickening is not rescued by expression of *35Spro:MYB26* in the *nst1nst2* background (arrow). H, Increased levels of anther endothecium thickening were, however, seen with the *35Spro:MYB26* in the *nst1nst1Nst2nst2* heterozygous background (arrow). I to L, Secondary thickening in the inflorescence stems (I) wild type, (J) *nst1nst2* double mutant (thickening is slightly reduced), and (K) the *nst1nst2* double mutant expressing *35Spro:MYB26*. L, Ectopic secondary thickening is seen in the inflorescence stem (arrows) when *MYB26* is overexpressed in presence of *NST2* (*35Spro:MYB26* in the *nst1nst1NST2nst2* heterozygous background). M, qRT-PCR expression analysis of *MYB26*, *NST1*, *NST2*, and *NST3* in the whole

enhanced in the wild-type background (Fig. 6, N and O), confirming that the observed phenotypic changes correlated with levels of *NST1/2* expression, whereas lines carrying the *35Spro:NST1* or *35Spro:NST2* constructs in the *myb26* or *ms35gl* mutant background showed a much-reduced level of *NST1* or *NST2* expression, as appropriate to the transgene (Fig. 6, N and O; Supplemental Fig. S1, R and S). This was observed in multiple lines and with both *NST1* and *NST2* constructs and therefore is unlikely to reflect position effects in the different overexpression lines. Given that in these lines the expression of the *NST1* and *NST2* genes is under regulation of the *CaMV35S* promoter, the low level of *NST1* and *NST2* observed may be the consequence of posttranscriptional regulation or direct or indirect action of the MYB26 protein on the stabilization of the *NST1/NST2* RNA.

NST1 and *NST2* Cannot Induce High-Level Expression of Genes Involved in the Biosynthesis of Secondary Thickening in the *myb26* Background

In wild-type lines carrying the *35Spro:NST1* or *35Spro:NST2* construct, an up-regulation of genes involved in wall biosynthesis was observed. This was particularly evident for cellulose (*IRX1* and *IRX3*) and hemicellulose (*FRAGILE FIBER8* [*FRA8*], *IRX8*, and *IRX10*) biosynthesis genes. Genes associated with lignin formation, *IRX4*, and *COMT* however, did not show a major change, although *IRX12* showed slight up-regulation (Supplemental Fig. S2). This up-regulation was more pronounced in lines carrying the *35Spro:NST1* transgenes than those with *35Spro:NST2*. It was observed that *NST1* was more effective in initiating ectopic secondary thickening than *NST2*; with high levels of *NST1* showing extensive secondary thickening in epidermis and endothecium, while high levels of *NST2* caused enhanced thickening in the endothecium (Fig. 6, I and K; Supplemental Fig. S1, J and N, and L and P); however, this was only seen when there was expression of *MYB26*. In the wild-type background, there was a direct correlation between the levels of *NST1/2* gene expression, enhanced expression of the secondary thickening biosynthesis genes (Supplemental Figs. S1 and 2), and the formation of increased secondary thickening (Fig. 6; Supplemental Fig. S1); however, this induction appears to be dependent on the presence of MYB26. In the wild-type background, ectopic thickening by NST1 overexpression was linked to high levels of *NST1* expression, with a cut off point of expression (~8× normal expression) not having ectopic thickening (Supplemental Fig. S3). This suggests that although NST1 and NST2 are both able to induce the expression of genes associated with secondary wall biosynthesis, NST1 is more effective, agreeing with previous observations made by Mitsuda et al. (2005). However, in the *myb26* mutant background, no enhancement of expression of these secondary wall biosynthesis genes was observed, regardless of whether *NST1* or *NST2* was expressed, and despite the fact the respective overexpression lines have higher expression compared to wild type (Supplemental Fig. S1, R and S).

Overexpression of Both *NST1* and *NST2* Together Can Induce Ectopic Thickening in the Anther Epidermis in the *myb26* Background

The *NST1* and *NST2* genes appear to act redundantly in the anther to regulate secondary thickening (Mitsuda et al., 2005), with expression of either *NST1* or *NST2* sufficient to induce secondary thickening. However, expression of either individually under the *CaMV35S* promoter was not able to complement the *myb26* mutation or induce significant secondary thickening. Despite the fact that NST1 and NST2 are able to function independently, we also tested both transgenes in combination to determine whether together they were able to affect anther secondary thickening. Overexpression of both *NST1* and *NST2* together in the *MYB26myb26* background resulted in increased secondary thickening in the anther endothecium and also ectopic anther filament and some epidermal thickening (Fig. 7, A and B). These lines were fertile since endothecium thickening was present and the ectopic epidermal thickening was at a low level, such that it did not prevent dehiscence. However, expression of both transgenes in the *myb26* mutant background had a surprising effect—anther endothecium thickening failed to develop, but extensive ectopic thickening in the anther epidermis occurred (Fig. 7, C and D). These lines failed to dehisce and were male sterile due to the lack of endothecium thickening, but also because of the ectopic anther epidermal thickening. The native endothecium thickening and the ectopic epidermal thickening forms across the cell length of the cells; however, the anther epidermal cells are arranged in a different orientation (along the anther length opposed to those of the endothecium, which form along the anther width; Kelliher and Walbot, 2011). Therefore, the thickening forms in the alternate (crossed) orientation to that of the endothecium. This means that as the anther dehydrates, it is still unable to open. This effect of indehiscence as a consequence of alternate thickening due to the orientation of the epidermal cells preventing dehiscence was also previously

Figure 4. (*Continued.*)
inflorescence of wild type, *nst1nst2* mutant, *nst1nst2* mutant expressing *35Spro:MYB26*, and in the *nst1* single mutant (*nst1nst1NST2nst2* heterozygous line), and *nst1nst1NST2nst2* heterozygous line expressing *35Spro:MYB26*. N, qRT-PCR expression of genes involved in secondary thickening pathways in the whole inflorescence of various backgrounds shown in M. Error bars represent SD in M and N (*t* test statistical analysis compared to its relevant background for each line; $*P \leq 0.05$; $**P \leq 0.01$).

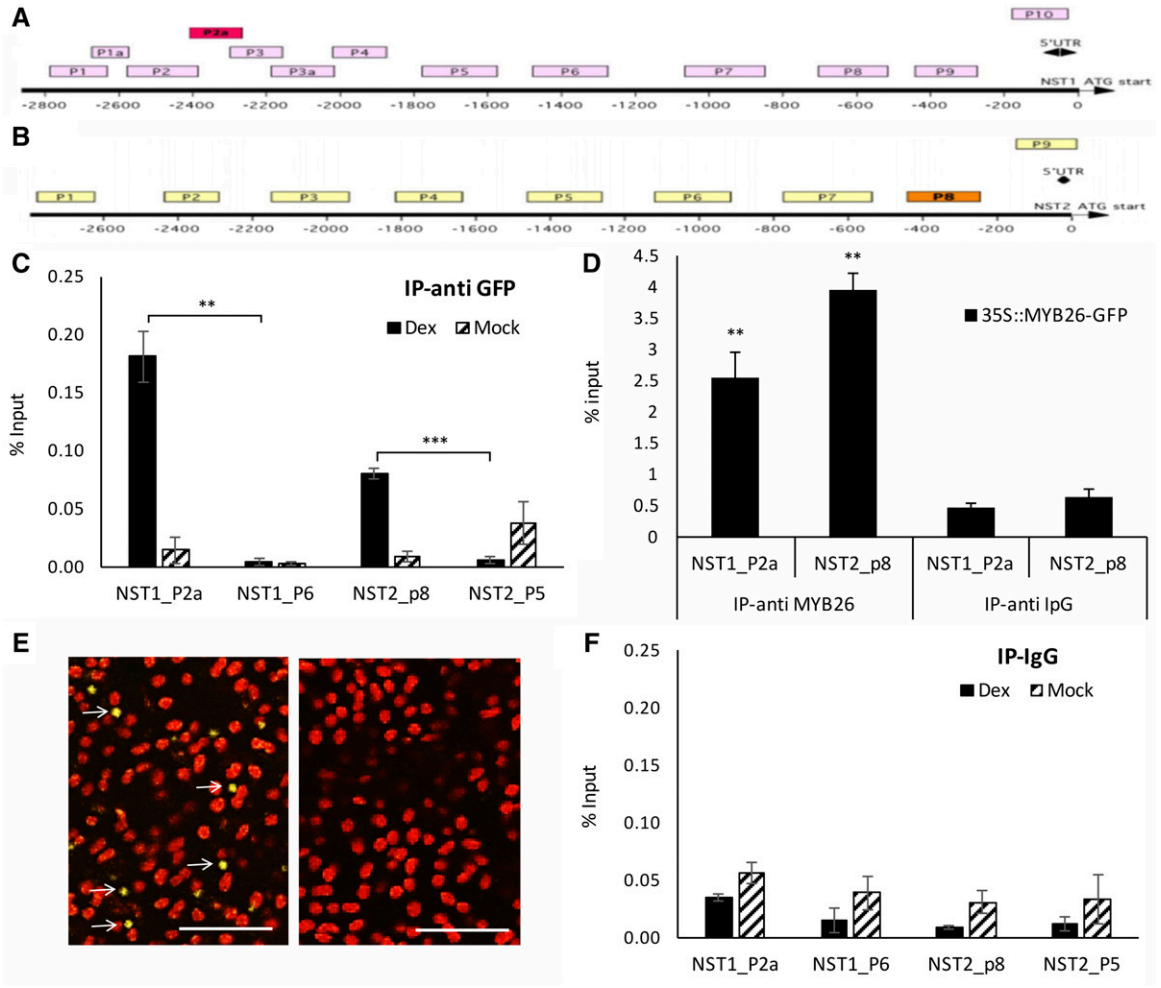

Figure 5. ChIP indicates that MYB26 directly binds to upstream regions of *NST1* and *NST2*. A and B, Diagram of upstream region of (A) *NST1* (B) *NST2*; boxes P1 to P10 indicate regions used for ChIP analysis; red/orange boxes are regions that showed positive binding. C and D, ChIP qPCR showing enrichment for (C) P2a in NST1 and P8 for NST2 using anti-GFP, and (D) anti-MYB26 antibodies. E, MYB26-YFP within the nucleus of the endothecium (left; arrows) was detected in the DEX-induced *MYB26pro:MYB26-GR-YFP* line; no nuclear localized expression was seen in the non-DEX-induced line (right). F, No ChIP qPCR enrichment was seen in the IP-ipG controls. Error bars represent SD (*t* test statistical analysis compared to control primer [C and F] or anti IpG [D] controls; $*P \leq 0.05$; $**P \leq 0.01$; $***P \leq 0.001$).

observed in wild-type lines overexpressing *MYB26* (Yang et al., 2007). Mutants of *MYB26* were previously observed to have changes in the cell expansion of the endothecium layer (Dawson et al., 1999; Yang et al., 2007); this may be as a consequence of MYB26 acting on other factors to induce cell differentiation or by it repressing a repressor to allow endothecium expansion and development. *NST1/2* do not appear to play a role in this, since when overexpressed, either individually or in combination, the endothecium and, in the case of ectopic expression, the other cell layers appeared contorted and failed to expand.

qRT-PCR expression analysis indicated that high levels of *NST1* and *NST2* expression were seen in lines expressing both transgenes and that this was effective in inducing *IRX1* and *IRX3*, downstream genes linked to cellulose biosynthesis, and also *FRA8*, associated with hemicellulose formation (Supplemental Fig. S4). *NST2* expression was high in both the *myb26* mutant and heterozygous *myb26MYB26* lines; however, this did not equate to secondary thickening formation, except where *MYB26* was present or when high levels of *NST1* were also present. The levels of downstream gene expression did not appear to directly correlate with levels of secondary thickening. The low changes in gene expression observed are likely to be a consequence of the very limited numbers of cells forming thickening in these lines, and therefore cell-by-cell changes may be masked.

Expression of *MYB26* under the Regulation of the *NST2* Promoter Rescues Fertility in the *myb26* Mutant

The *NST2* promoter has been shown to be expressed in the floral tissues (Mitsuda et al., 2005); we confirmed this by using an *NST2pro:GUS* transgenic line (Fig. 8A).

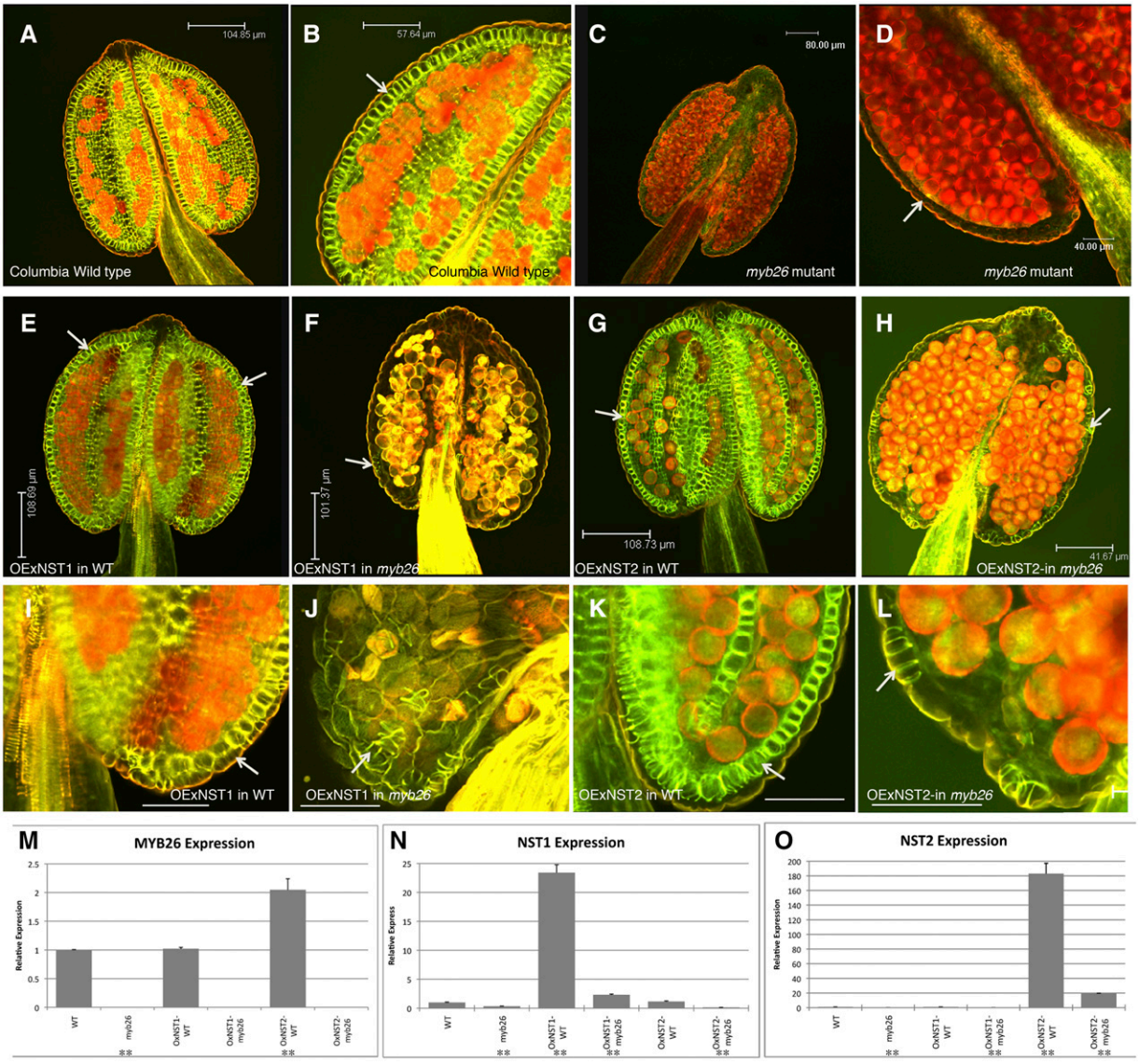

Figure 6. Expression of *NST1* or *NST2* under the control of the *CaMV35S* promoter is unable to rescue anther secondary thickening in the *myb26* mutant. A to L, Anthers stained for secondary thickening with acridine orange/ethidium bromide and visualized by confocal microscopy. A and B, Wild-type anther showing endothecium thickening (arrow). C and D, *myb26* mutant lacking endothecium thickening (arrow). E and I, Overexpression of *NST1* (*35Spro:NST1*) in wild-type background; increased levels of secondary thickening are seen in both the endothecium and epidermal tissues (arrows). F and J, Overexpression of *NST1* (*35Spro:NST1*) in the *myb26* mutant background; occasional patches of secondary thickening are seen in the epidermal tissues (arrow), but these are extremely limited, and no endothecium thickening is seen. G and K Overexpression of *NST2* (*35Spro:NST2*) in wild-type background; increased levels of secondary thickening are seen in the endothecium (arrow), but not in the epidermal tissues as seen with *NST1* overexpression in wild type. H and L, Overexpression of *NST2* (*35Spro:NST2*) in the *myb26* mutant background; occasional patches of secondary thickening are seen in the epidermal cells (arrow); however, these are extremely limited, and the endothecium cells are abnormal and lack the usual expansion seen in these cells prior to secondary thickening deposition. I to L are higher magnifications of the same anther shown in E to H. Scale bars represent 104.85 μm in A, 57.64 μm in B, 80 μm in C, 50 μm in D, 108.69 μm in E, 101.37 μm in F, 108.73 μm in G, 41.67 μm in H, and 50 μm in I to L. M to O, Expression by qRT-PCR analysis in the wild type, *myb26* mutant, and overexpression lines of (M) *MYB26*, (N) *NST1*, and (O) *NST2*. Error bars represent SD (*t* test statistical analysis compared to its relevant background for each line; $^{**}P \leq 0.01$).

Expression was observed in the young postmeiotic anthers, older filaments, and pollen around the time of filament extension, prior to dehiscence. This construct was introgressed into the *myb26* mutant; the expression pattern was as seen for the wild type (Fig. 8B), indicating that *NST2* is induced by some other factor in addition to MYB26. We subsequently expressed *MYB26* under the control of the *NST2* promoter; the transgenic

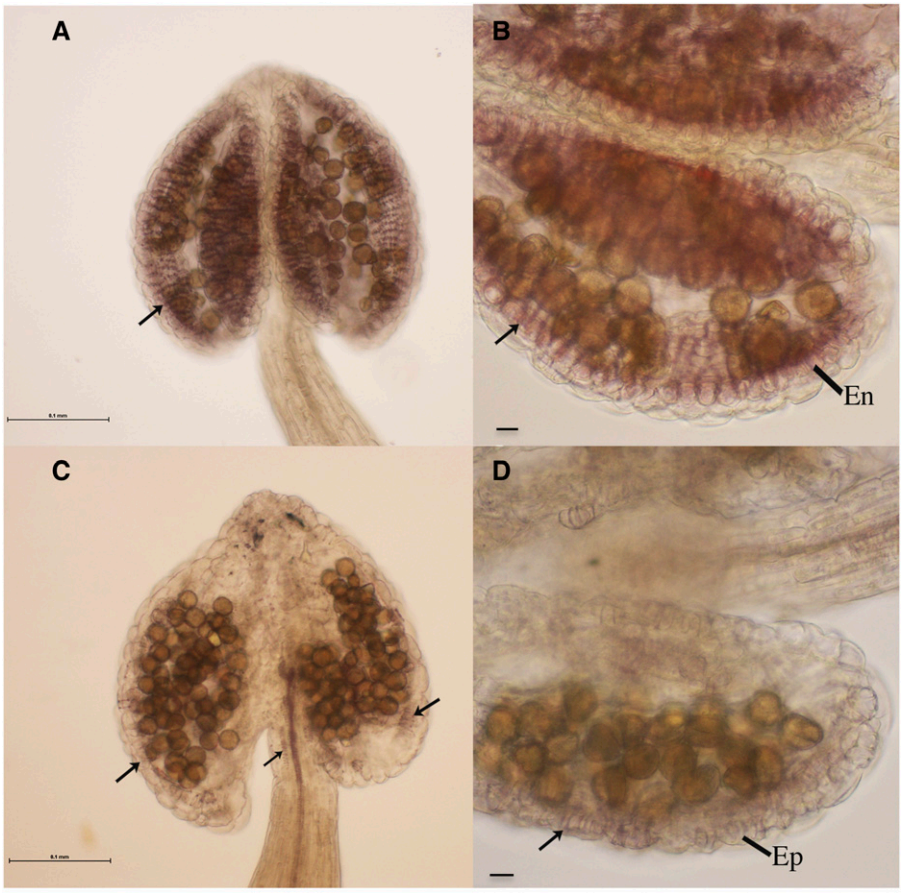

Figure 7. Anthers from *MYB26myb26* heterozygotes and *myb26* mutants that are expressing both *NST1* and *NST2* under the control of the *CaMV35S* promoter. A to D, Anthers isolated and stained with phloroglucinol HCl to detect lignified thickening from lines overexpressing both *NST1* and *NST2*. A and B, High levels of native secondary thickening are seen in the endothecium (En) layer (arrows) in the *MYB26myb26* heterozygote background with both *NST1* and *NST2* transgenes. C and D, In the *myb26* mutant the anthers appear contorted with ectopic thickening in epidermal tissues (arrows shows ectopic thickening in anther epidermis [Ep] and also in the filament); normal secondary thickening is not seen in the endothecium in the *myb26* background, regardless of expression of both *NST1* and *NST2*. Scale bar represents 0.1 mm.

line showed complete rescue and full fertility in the *myb26* mutant. This confirms that a factor additional to *MYB26* is switching on expression of *NST2*, since expression is still observed in the *myb26* mutant. Analysis of secondary thickening in these anthers showed that ectopic thickening formed in the endothecium and also in the filament (Fig. 8, D, G, and J). The thickening in these transgenic lines was increased as compared to the wild-type lines; this was expected since expression of *MYB26* would result in a feedback loop that enhanced expression of both *NST2* and *NST2pro:MYB26*, thus resulting in enhanced expression and secondary thickening in areas where *NST2* expression was initially occurring. The deposition of thickening in the anther and filament confirms the GUS expression pattern of *NST2*; the lack of epidermal thickening indicates that functional NST2 is not present in the anther epidermis.

Neither NST1 nor NST2 Interacts with MYB26 in Yeast

The full-length cDNA of *MYB26*, *NST1* and *NST2* were cloned into the Yeast two-hybrid pDEST22 Activation domain (AD) vector and pDEST32 DNA Binding domain (DB) vector (Invitrogen). These were used in pairwise combinations in yeast strain MaV203 and analyzed for activation of the expression of the three reporter genes (*HIS3*, *URA3*, and *lacZ*). A low level of autoactivation was seen with *MYB26* fused to the DB domain, which could be overcome using at least 50 mM 3-amino-1,2,4-triazole; however, relatively strong autoactivation was also observed from the *NST2* equivalent clone. Nevertheless, combinations of MYB26 as bait (DB) with NST1, or NST2 as prey (AD), suggest that there is no interaction occurring between the NST1 or NST2 proteins and MYB26 (Supplemental Fig. S5); however, MYB26-MYB26 may form as a homodimer, and homo- and heterodimerization of NST1 and -2 is also likely to occur, as predicted from the NAC domain structure (Olsen et al., 2005).

DISCUSSION

MYB26 Expression Regulates Tissue-Specific Localization of Secondary Thickening in the Anther Endothecium

MYB26, NST1, and NST2 initiate secondary thickening in the anther by a complex pathway that involves multiple regulatory points. The specific cellular localization of this thickening is critical for efficient anther opening. Our data indicate that the expression of MYB26 is essential to the formation and spatial arrangement of

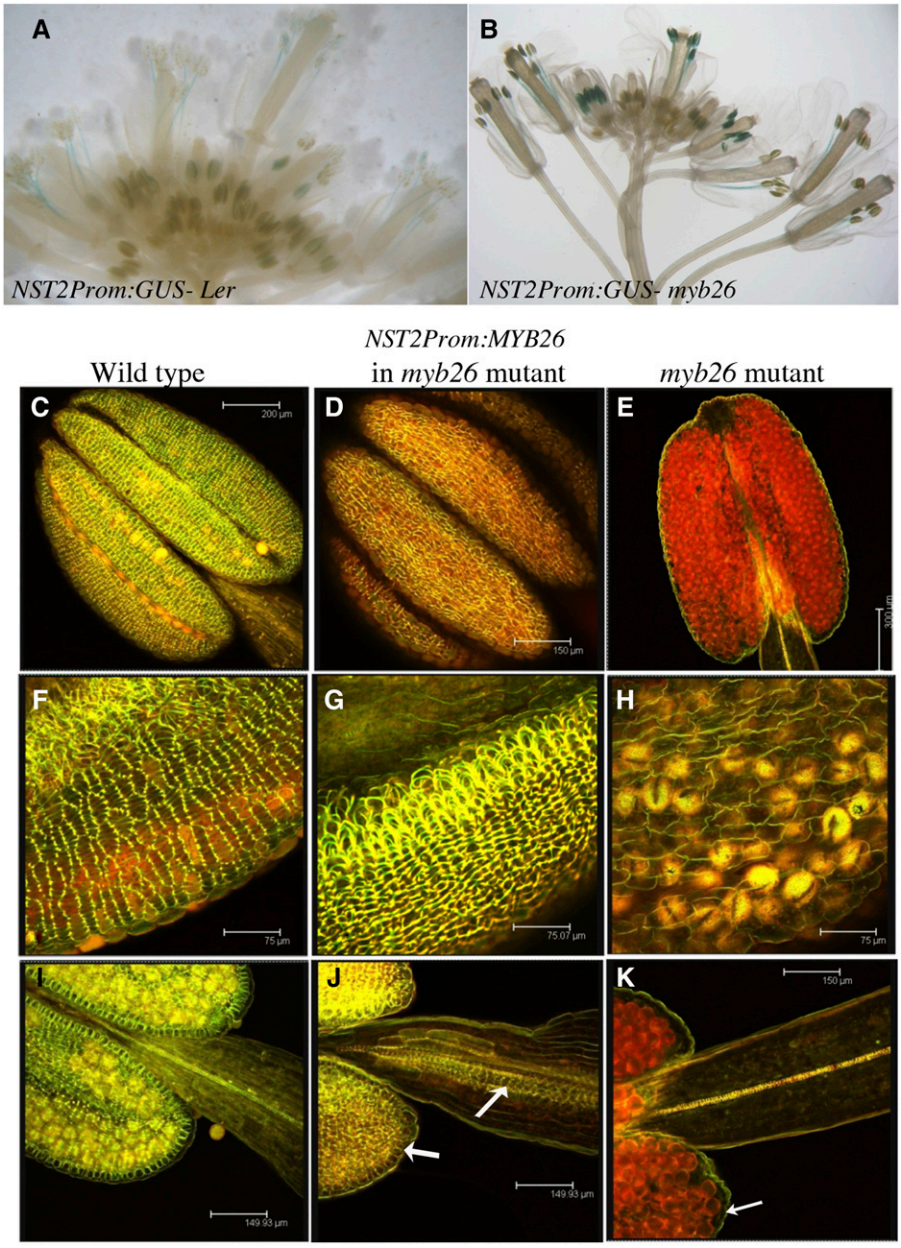

Figure 8. Rescue of fertility in the *myb26* mutant by expression of *MYB26* regulated by the *NST2* promoter. A, *NST2pro:GUS* expression in wild type, showing expression in extending filaments prior to dehiscence, and in postmeiotic anthers. B, *NST2pro:GUS* expression in the *myb26* mutant, showing expression in extending filaments prior to dehiscence, and in postmeiotic anthers. C to K, Stamen stained for secondary thickening with acridine orange/ethidium bromide and visualized by confocal microscopy; (C, F, and I) wild-type anthers and filaments; (D, G, and J) *NST2pro:MYB26* expression in the *myb26* mutant showing high levels of secondary thickening in the endothecium and increased secondary thickening in the filament; (E, H, and K) *myb26* mutant with no thickening in the anther endothecium. Scale bars represent 200 μm in C, 150 μm in D, 300 μm in E, 75 μm in F to H, and 150 μm in I to K.

secondary thickening in the anther and that it acts via induction of NST1 and NST2. Nevertheless, it is clear that although the NAC domain genes are required for induction of secondary thickening biosynthesis, they are only able to do this if MYB26 is present, implying an additional regulatory step that is controlled by MYB26 that is required for progression of the tissue-specific secondary thickening in the anther.

Using a functional, inducible MYB26-YFP fusion protein, we have shown the MYB26 protein shows specific targeted localization that is different from the MYB26 transcript (Fig. 2). Previously, we reported that *MYB26* expression, determined using a *MYB26pro:GUS* construct, was observed in many floral tissues, including the nectaries, style, filaments, and anthers (Yang et al., 2007). However, the MYB26 protein shows specific localization to the anther endothecium (Fig. 2), which agrees with the phenotype seen in the *myb26/ms35* mutants, with defects in the anther endothecium, rather than alterations in the style and other floral tissue (Dawson et al., 1999; Steiner-Lange et al., 2003; Yang et al., 2007). This suggests that posttranscriptional or translational regulation of *MYB26* is occurring, which confines MYB26 protein to the endothecium layer. In addition, activation by nuclear localization of the functional MYB26-GR-YFP protein after DEX treatment resulted in a decrease of *MYB26* transcript (Fig. 2D), suggesting that the MYB26 protein may down-regulate its own expression. The presence of the MYB26-YFP protein was also only seen for a limited period after DEX treatment, implying rapid turnover of

the MYB26 protein (data not shown). An F-box gene, *Secondary wall thickening-Associated F-box1* (*SAF1*) has recently been reported to negatively regulate endothecium secondary thickening, which, when overexpressed, results in defective endothecium thickening and indehiscence (Kim et al., 2012). It may be that SAF1, or another factor, may act by targeting the breakdown of MYB26, or NST1/2, and preventing accumulation of these proteins and thus secondary thickening gene expression.

Gene Expression Network Associated with Secondary Thickening in the Anther

The genetic evidence suggests that *MYB26* acts upstream of *NST1/2*, since *MYB26* overexpression was unable to rescue the *nst1nst2* double mutant (Fig. 4), and *MYB26-GR* was able to induce expression of *NST1* and *NST2* (Fig. 3). This appears to be via direct regulation, with MYB26 binding to both promoters by ChIP-PCR (Fig. 5) and rapid induction (within 4–6 h) of *NST1/2* seen after DEX activation of MYB26. However, *NST2* also appears regulated by an additional factor(s), since the *NST2* promoter can drive gene expression in the *myb26* background, as demonstrated by the *NST2pro:GUS* and *NST2pro:MYB26* constructs (Fig. 8). In the absence of *myb26*, *NST2* appears to show similar expression within the endothecium, as indicated by the rescue of fertility and endothecium thickening by *NST2:MYB26*; nevertheless, MYB26 is essential for induction of endothecium secondary thickening.

In the wild-type or *MYB26myb26* heterozygous background, overexpression of *NST1* led to increased secondary thickening within the endothecium and ectopic secondary thickening in the epidermis. However, in the *myb26/ms35* mutant, overexpression of *NST1/2* singularly or combined did not result in secondary thickening within the endothecium and therefore was unable to rescue the *myb26/ms35* mutants (Figs. 6 and 7; Supplemental Fig. S1). This is unlikely to be a consequence of the promoter since *35Spro:MYB26* was previously able to rescue fertility in the *myb26* mutant (Yang et al., 2007). Nevertheless, combined overexpression of *NST1* and *NST2* resulted in ectopic thickening in the anther epidermis in the *myb26* mutant, but endothecium thickening still did not occur. It therefore appears that it is easier for the epidermis to form ectopic thickening than other cell layers in the anther. Epidermal tissues have been reported as highly metabolically active (Mahroug et al., 2006). The ability of the epidermis to develop thickening if *NST1* expression is sufficiently high may be a reflection of the enhanced competency of this tissue for such metabolic activity. NST1 is more effective at inducing secondary thickening biosynthesis (Mitsuda et al., 2005); therefore, this may explain why overexpression of *NST2* in the wild-type background is unable to induce epidermal thickening.

This lack of rescue appears to be at least partly due to the insufficient expression of *NST1* and *NST2* in the absence of MYB26, as *35Spro:NST1* and *35Spro:NST2* expression was reduced in the *myb26/ms35* mutants in comparison to overexpression within the wild-type background (Supplemental Fig. S3). The relationship among MYB26 and NST1 and NST2 is therefore more complex than a linear network. It appears that an additional factor(s) controlled by *MYB26* enables an increase of the *NST1* and *NST2* transcripts and thus induction of secondary thickening genes. This could be a consequence of altered stability of the NST1/2 transcripts/proteins, or of the removal of an additional repressor facilitating transcript increase, which facilitates secondary thickening formation (Fig. 9). This additional role of MYB26 does not appear to be a consequence of direct interactions at the protein level, since NST1/NST2 and MYB26 do not appear to interact in a yeast two-hybrid analysis (Supplemental Fig. S5).

In the absence of MYB26, secondary thickening can only be achieved in the anther if both *NST1* and *NST2* are expressed at high levels and then only ectopically in the wrong cell layer, the epidermis. This suggests that there is a highly cell-specific, spatial regulation of thickening involving MYB26, which is easier to overcome in the epidermis than in other cell layers in the anther, in particularly the endothecium. NAC domain genes are a large group of plant-specific transcription factors that show specific regulation, by various mechanisms, including miRNA cleavage and ubiquitin-mediated proteolysis (Olsen et al., 2005). For example *NAM*, *CUC1*, and *CUC2*, which function in shoot meristem formation and boundary specification, are regulated by miRNAs (Aida et al., 1997). It can be speculated that similar regulation of *NST1* and *NST2* may be occurring via miRNAs, which may be repressed by MYB26. The F-box protein Secondary wall thickening-Associated F-box 1 (SAF1) could also potentially be regulating the protein turnover of NST1/2, since when this is overexpressed it negatively regulates endothecial secondary wall thickening (Kim et al., 2012). This also agrees with the observation that *SAF1* is up-regulated in the *myb26* mutant (https://www.cpib.ac.uk/anther; Pearce et al., 2015). The WRKY12 transcription factor has also been shown to negatively regulate *NST2* (Wang et al., 2010), and Homeobox-leucine zipper protein 15 (AtHB15) negatively regulates *NST3* and *NST2* within pith parenchyma cells (Du et al., 2015). WRKY13, however, positively regulates *NST1–3* within the stem and has been shown to bind directly to the *NST2* promoter (Li et al., 2015). It is therefore possible that there is a similar transcription factor regulating expression or turnover of *NST1* and *NST2* within the anther cell layers. In wild-type plants transcription factor (TCP24) is strongly expressed in the early stages of endothecium formation, and this expression reduces and eventually disappears by the time secondary wall thickening occurs (Wang et al., 2015). TCP24, which is regulated by miR139, has been shown to repress endothecium secondary thickening and *NST1/2* expression, but not *MYB26* (Wang et al., 2015); however, it does not appear to show significant

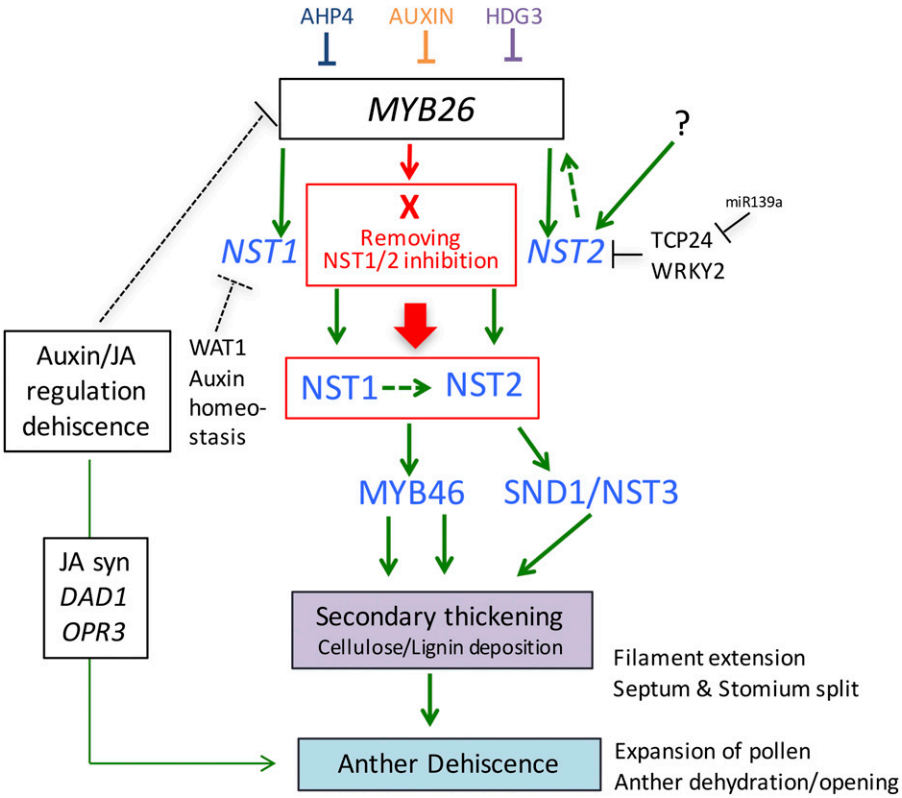

Figure 9. Model of MYB26 regulation of anther secondary thickening pathway. MYB26 regulation of secondary thickening through downstream the redundant transcription factors NST1/NST2. Arrows represent direct regulation, while bar represents repression, and dotted lines represent predicted regulation/repression. X = unknown factor that enables NST1/2 to initiate secondary thickening. This could be via NST1/2 protein activation/stabilization or removal of an inhibitor involved in NST1/2 degradation/turnover. AHP4, ARABIDOPSIS HISTIDINE-CONTAINING PHOSPHOTRANSFER FACTOR 4; HDG3, HOMEODOMAIN GLABRA 2-LIKE PROTEIN 3; TCP24 and WRKY2, transcription factor; JA, Jasmonic Acid; DAD1, DEFECTIVE IN ANTHER DEHISCIENCE1; OPR3, 12-OXOPHYTODIENOATE REDUCTASE 3; WAT1, WALLS ARE THIN1.

expression changes in the *myb26* mutant (https://www.cpib.ac.uk/anther; Pearce et al., 2015).

Lack of *NST1*/*NST2* Alters Plant Stature alongside Regulating Secondary Thickening

The *nst1nst2* double mutant shows altered stature, with a very bushy appearance, which is rescued by the presence of a single copy of either the *NST1* or *NST2* gene (Mitsuda et al., 2005). This phenotype is not seen with the *myb26* mutant (Dawson et al., 1999; Steiner-Lange et al., 2003), suggesting that this is not associated with reduced fertility but may reflect the lack of *NST1* and *NST2* expression throughout the plant. A similar phenotype was reported for the *saf1* mutant, and it was suggested that this may be a consequence of altered auxin levels, which is also seen when flavonoid balance is altered (Kim et al., 2012). This phenotype is not seen in the *nst1nst1NST2nst2* lines, suggesting that a single copy of *NST2* is able to compensate for the lack of NST1 in the plant. Recently, it has been shown that *NST2* together with *NST1* and *NST3* regulate secondary cell wall synthesis in fibers of stems (Zhong and Ye, 2015). qRT-PCR expression analysis in the different transgenic mutant lines indicated that when expressed at very high levels *NST2* may alter the level of expression or enhance the stability/reduce the turnover of the *MYB26* and *NST3* transcripts (Figs. 4 and 6M). However, *NST1* does not appear to affect the expression levels of either *MYB26* or *NST2* (Figs. 6 and 9).

Expression of Secondary Thickening Biosynthesis Genes Is Regulated by *NST1/2*

Overexpression of *MYB26* in the wild-type background resulted in increased thickening in the endothecium, epidermis, and ectopically throughout the plant; however, it was unable to induce lignin and cellulose biosynthesis genes in the absence of *NST1/2* (Fig. 4N) and appears to act by directly up-regulating expression of both *NST1/2*, which in turn regulates cellulose biosynthesis (particularly *IRX1* and *-3*) and lignin biosynthetic genes. *NST1/2* act redundantly, and presence of one of them was sufficient for secondary thickening induction. Nevertheless, it appears that secondary thickening biosynthesis is principally mediated via NST1, with NST1 more effective in the induction of secondary thickening biosynthesis genes, as previously reported (Mitsuda et al., 2005). However qRT-PCR data suggests that NST2 may also indirectly cause up-regulation of *NST1* via a feedback loop of up-regulation of *MYB26* (Fig. 9).

Studies of the *NST2-NST3/SND1* and *VND1–VND7* genes suggest that secondary cell wall regulating NAC-domain genes are all able to directly bind targets associated with cellulose, lignin, and hemicellulose biosynthesis, through a 19-bp consensus sequence secondary wall NAC-binding element (Zhong et al., 2010; Yamaguchi et al., 2011; Taylor-Teeples et al., 2015). Complementation studies have shown that by misexpression of one NAC-domain gene is able to rescue the mutant phenotype, indicating that these genes are functional

paralogs (Zhong et al., 2010; Yamaguchi et al., 2011; Zhong and Ye, 2014). Almost all of these transcription factors contain at least one secondary wall NAC-binding element site in their own promoter (except VASCULAR-RELATED NAC-DOMAIN 6 [*VND6*]; Zhong and Ye, 2014), and *NST3* has been shown to up-regulate its own expression (Wang et al., 2011). Given the observed similarities between the NAC domain genes that regulate secondary thickening in different plant tissues, it seems likely that *NST1* may also be able to up-regulate its own expression.

CONCLUSION

Overall, it appears that there is tight regulation of secondary thickening in the anther, which is controlled by localization of the MYB26 protein to the endothecium cell layer and direct induction of *NST1* and *NST2* expression by MYB26 (Fig. 9). However, there is an additional mechanism involving MYB26 that enables the accumulation of the NAC domain transcripts that is essential for thickening. This may be needed to maintain cell specificity, since other factors are also involved in the activation of these *NAC* domain genes, e.g. *NST2*, thereby facilitating strict temporal and boundary control to thickening. Such high-level cell-specific control is a prerequisite to effective regulation of dehiscence at optimal developmental stages.

MATERIALS AND METHODS

Plant Materials and Growth Conditions

Two Arabidopsis (*Arabidopsis thaliana*) *MYB26* mutant lines were used as previously described by Yang et al. (2007); the x-ray line *ms35gl* (Z.A.W. lab, University of Nottingham) and the *myb26* T-DNA SALK line (SALK_112372) (SIGnal; Alonso et al., 2003), as well as the T-DNA SALK lines *nst1*, *nst2*, and *nst1nst2* double mutants previously described by Mitsuda et al. (2005). T1 seeds of *NST2pro:GUS myb26* (SALK 112372; CR684), *NST1pro:GUS myb26* (DR0561), *NST2pro:MYB26 myb26* (DR0562), and *35Spro:MYB26 NST1*pro:GUS (DR0816) were generated by Dr. Nobutaka Mitsuda (National Institute of Advanced Industrial Science and Technology, Tsukuba, Japan). Plants were selected on hygromycin/kanamycin plates, as appropriate, then transferred into Levington M3 (The Scotts Company) compost supplemented with 0.2 g L-1 of Intercept 70 WG (Scotts, Monro South) and grown in a glasshouse at 21°C/17°C (day/night) and 22/2 h photoperiod as previously described (Dawson et al., 1999), along with their appropriate wild-type controls (ecotype Heynh. var Landsberg *erecta* [L*er*] for *ms35gl*; and ecotype Columbia [Col-0] for *myb26* SALK line).

DEX-Inducible MYB26 Construct

A 5-kb region of *MYB26* including a 3-kb upstream region was amplified from genomic DNA of L*er* using primers MS35prom-*Kpn*I and MS35cDNA-R-*Spe*I (Supplemental Table S1) and then cloned into TOPO PCR Blunt II (Invitrogen). The fragment was then digested with *Kpn*I/*Spe*I and cloned into *pGREEN0229-GR-YFP* (kindly provided by the Bennett Lab, University of Nottingham) upstream of *GR-YFP* to produce the construct *pGREEN0229MYB26pro:MYB26-GR-YFP*. The construct was confirmed by PCR and sequencing, then transferred into *Agrobacterium* (GV3101 + pSOUP) by electroporation (Sambrook et al., 1989). Arabidopsis heterozygous *myb26* SALK mutant and *ms35gl* plants were transformed by floral dipping (Clough and Bent, 1998). The T1 generation were screened for Basta resistance and PCR tested for the transgene. These plants grew to flowering stage; the sterile plants with flower buds showing *myb26* mutant phenotype were sprayed with, or dipped into 25 μM DEX + 0.02% (v/v) Silwet L-77 solution. YFP was observed using confocal microscope (TCS SP2, Leica) with 514-nm excitation.

Overexpression Lines

The coding region of NST1 and NST2 with stop codons was amplified by PCR (Supplemental Table S1), cloned into pDONR211 (Invitrogen), and then transferred by Gateway cloning into the PGWB5 (Invitrogen) destination vector to form *35Spro:NST1* and *35Spro:NST2* overexpression constructs. The constructs were then transferred into *Agrobacterium* (C58) by electroporation (Sambrook et al., 1989) and transformed into Arabidopsis heterozygous *myb26* SALK line and heterozygous *ms35glMS35* plants by floral dipping (Clough and Bent, 1998). The T1 generation were screened for hygromycin resistance and PCR tested for the transgene (Supplemental Table S1). The selected homozygous lines of *35Spro:NST1* and *35Spro:NST2* in the heterozygous *myb26MYB26* and *ms35glMS35* background were then subsequently crossed to produce an overexpression of both *NST1* and *NST2* lines in the homozygous *myb26* and *ms35* background.

Expression Analysis

RNA was isolated from buds and leaves (RNeasy, Qiagen) and cDNA prepared using 5 μg total RNA in a 20 μL reaction (Superscript II reverse transcriptase, Invitrogen). qRT-PCR was carried out using a Light Cycler (Roche) in a 384 plate using the Maxima SYBRR Green QPCR Master Mix in a final volume of 9 μL containing 0.2 μL of cDNA and 0.2 μL of the appropriate primers (Supplemental Table S1). PCR cycling conditions for amplification were 95°C for 10 min, then 40 cycles of 95°C for 30 s, 58°C for 1 min, and 72°C for 1 min. All samples were run at least in duplicate. Data acquisition and analyses were performed using the Light Cycler software. Relative expression levels were determined in comparison to actin or PP2A expression using the $2^{-\Delta\Delta}C_T$ analysis method (Livak and Schmittgen, 2001).

Microscopy

For analysis of lignin, fresh samples were stained with phloroglucinol-HCl (Ruzin, 1999) and were observed under a light microscope (Nikon); for confocal microscopy (TCS SP2, Leica) observation a modified ethidium bromide/acridine orange stain was used (Yang et al., 2007). The ethidium bromide stains lignified cells (red fluorescence; 514 nm excitation; emission collection 590 nm [570–620 nm]) and the acridine orange stains lignified walls with a drop of fluorescence for nonlignified walls (green fluorescence; 488 nm excitation; emission collection 520 nm [510–530 nm]). A minimum of ten independent transformants were analyzed.

Yeast Two-Hybrid Analysis

A yeast two-hybrid screen was conducted using the Gateway yeast two-hybrid system (Invitrogen) according to the manufacturer's instructions. The full-length *MYB26*, *NST1*, and *NST2* coding regions were cloned into pDEST32 (DNA DB) and pDEST22 (AD) vectors and used to check pairwise interactions in yeast strain MaV203 carrying three reporter genes (*HIS3*, *URA3*, and *lacZ*). Interactions and autoactivation were tested by His selection supplied with 30, 60, and 80 mM of 3-Amino-1,2,4-triazole and X-Gal assay, following the manufacturer's instructions. Control assays were used as positive and negative controls for the analysis; these consisted of empty pDEST22 and pDEST32 (A—negative control for growth); pEXPTM22/RalGDS-m2 and pEXPTM32/Krev1 (B—negative control for interaction); pEXPTM22/RalGDS-m1 and pEXPTM32/Krev1 (C—weak positive control for interaction); pEXPTM22/RalGDS-wt and pEXPTM32/Krev1 (D—strong positive control for interaction). They were used as described by the manufacturer's instructions.

ChIP Analysis

ChIP analysis was conducted on MYB26-DNA complexes in the *35Spro:MYB26-GFP*, and DEX-inducible *MYB26pro:MYB26-GR-YFP* line using both a peptide-derived anti-MYB26 antibody and ChIP grade anti-GFP (Abcam; ab290, 3%–5% [v/v] final concentration), respectively. Following a modified protocol from Ferguson et al., (2017), chromatin was isolated from 5 g bud tissue. All samples were run in triplicate with at least two biological replicates.

Negative controls were as follows, noninduced *MYB26pro:MYB26 GR YFP* line (treated with water rather than DEX), nonspecific antibody (anti-HA or anti-HIS IgG), and negative promoter primers (NST1-P6 and NST2-P5) were used. Primers for qChIP-PCR are shown in Supplemental Table S1. Data are presented as %input to test whether there was enrichment of the *NST1* and *NST2* promoters in comparison to all the controls used.

Accession Numbers

Arabidopsis Genome Initiative locus identifiers for the genes mentioned in this article are as follows: *MYB26* (At3g13890, Q9SPG3); *NST1* (At2g46770 Q84WP6); *NST2* (At3g61910, Q9M274); *SND1* (AT1G32770, Q9LPI7); *VND7* (AT1G71930, Q9C8W9); *IRX1* (At4g18780, Q8LPK5); *IRX3* (At5g17420, Q9SWW6); *FRA8* (AT2G28110, Q9ZUV3); *IRX8* (At5g54690, Q9FH36); *IRX10* (At1g27440, Q9FZJ1); *IRX4* (At1g15950, Q9S9N9); *IRX12* (At2g38080, O80434); *COMT* (At1g67980, Q9C9W3).

Supplemental Data

The following supplemental materials are available.

Supplemental Figure S1. Expression of *NST1* or *NST2* under the control of the *CaMV35S* promoter is unable to rescue anther secondary thickening in the *ms35* mutant.

Supplemental Figure S2. qRT-PCR expression and secondary thickening analysis of *NST1* in wild-type and *ms35* mutant buds overexpressing *NST1*.

Supplemental Figure S3. Ectopic expression of *NST1* under the control of *CaMV35S* promoter is proportional to the level of *NST1* expression.

Supplemental Figure S4. qRT-PCR expression analysis in wild type and *myb26* mutant, and in *MYB26myb26* and *myb26myb26* lines overexpressing both *NST1* and *NST2*.

Supplemental Figure S5. No interactions are detected by yeast-two hybrid analysis between MYB26 and NST1, or MYB26 and NST2.

Supplemental Table S1. Primers used.

ACKNOWLEDGMENT

Seed stocks were provided by NASC.

Received June 8, 2017; accepted July 17, 2017; published July 19, 2017.

LITERATURE CITED

Aida M, Ishida T, Fukaki H, Fujisawa H, Tasaka M (1997) Genes involved in organ separation in Arabidopsis: An analysis of the cup-shaped cotyledon mutant. Plant Cell **9:** 841–857

Alonso JM, Stepanova AN, Leisse TJ, Kim CJ, Chen H, Shinn P, Stevenson DK, Zimmerman J, Barajas P, Cheuk R, et al (2003) Genome-wide insertional mutagenesis of *Arabidopsis thaliana*. Science **301:** 653–657

Ariizumi T, Toriyama K (2011) Genetic regulation of sporopollenin synthesis and pollen exine development. Annu Rev Plant Biol **62:** 437–460

Caffall KH, Pattathil S, Phillips SE, Hahn MG, Mohnen D (2009) *Arabidopsis thaliana* T-DNA mutants implicate GAUT genes in the biosynthesis of pectin and xylan in cell walls and seed testa. Mol Plant **2:** 1000–1014

Cecchetti V, Altamura MM, Brunetti P, Petrocelli V, Falasca G, Ljung K, Costantino P, Cardarelli M (2013) Auxin controls Arabidopsis anther dehiscence by regulating endothecium lignification and jasmonic acid biosynthesis. Plant J **74:** 411–422

Cecchetti V, Celebrin D, Napoli N, Ghelli R, Brunetti P, Costantino P, Cardarelli M (2017) An auxin maximum in the middle layer controls stamen development and pollen maturation in Arabidopsis. New Phytol **213:** 1194–1207

Clough SJ, Bent AF (1998) Floral dip: a simplified method for Agrobacterium-mediated transformation of *Arabidopsis thaliana*. Plant J **16:** 735–743

Dawson J, Sözen E, Vizir I, Van Waeyenberge S, Wilson ZA, Mulligan BJ (1999) Characterization and genetic mapping of a mutation (*ms35*) which prevents anther dehiscence in *Arabidopsis thaliana* by affecting secondary wall thickening in the endothecium. New Phytol **144:** 213–222

Dawson J, Wilson ZA, Aarts MGM, Braithwaite AF, Briarty LG, Mulligan BJ (1993) Microspore and pollen development in six male-sterile mutants of *Arabidopsis thaliana*. Can J Bot **71:** 629–638

Du Q, Avci U, Li S, Gallego-Giraldo L, Pattathil S, Qi L, Hahn MG, Wang H (2015) Activation of miR165b represses AtHB15 expression and induces pith secondary wall development in Arabidopsis. Plant J **83:** 388–400

Ferguson AC, Pearce S, Band LR, Yang C, Ferjentsikova I, King J, Yuan Z, Zhang D, Wilson ZA (2017) Biphasic regulation of the transcription factor ABORTED MICROSPORES (AMS) is essential for tapetum and pollen development in Arabidopsis. New Phytol **213:** 778–790

Kelliher T, Walbot V (2011) Emergence and patterning of the five cell types of the *Zea mays* anther locule. Dev Biol **350:** 32–49

Kim YY, Jung KW, Jeung JU, Shin JS (2012) A novel F-box protein represses endothecial secondary wall thickening for anther dehiscence in *Arabidopsis thaliana*. J Plant Physiol **169:** 212–216

Kubo M, Udagawa M, Nishikubo N, Horiguchi G, Yamaguchi M, Ito J, Mimura T, Fukuda H, Demura T (2005) Transcription switches for protoxylem and metaxylem vessel formation. Genes Dev **19:** 1855–1860

Li W, Tian Z, Yu D (2015) WRKY13 acts in stem development in *Arabidopsis thaliana*. Plant Sci **236:** 205–213

Livak KJ, Schmittgen TD (2001) Analysis of relative gene expression data using real-time quantitative PCR and the 2(-Delta Delta C(T)) method. Methods **25:** 402–408

Ma H (2005) Molecular genetic analyses of microsporogenesis and microgametogenesis in flowering plants. Annu Rev Plant Biol **56:** 393–434

Mahroug S, Courdavault V, Thiersault M, St-Pierre B, Burlat V (2006) Epidermis is a pivotal site of at least four secondary metabolic pathways in *Catharanthus roseus* aerial organs. Planta **223:** 1191–1200

Mitsuda N, Iwase A, Yamamoto H, Yoshida M, Seki M, Shinozaki K, Ohme-Takagi M (2007) NAC transcription factors, NST1 and NST3, are key regulators of the formation of secondary walls in woody tissues of Arabidopsis. Plant Cell **19:** 270–280

Mitsuda N, Ohme-Takagi M (2008) NAC transcription factors NST1 and NST3 regulate pod shattering in a partially redundant manner by promoting secondary wall formation after the establishment of tissue identity. Plant J **56:** 768–778

Mitsuda N, Seki M, Shinozaki K, Ohme-Takagi M (2005) The NAC transcription factors NST1 and NST2 of Arabidopsis regulate secondary wall thickenings and are required for anther dehiscence. Plant Cell **17:** 2993–3006

Nelson MR, Band LR, Dyson RJ, Lessinnes T, Wells DM, Yang C, Everitt NM, Jensen OE, Wilson ZA (2012) A biomechanical model of anther opening reveals the roles of dehydration and secondary thickening. New Phytol **196:** 1030–1037

Olsen AN, Ernst HA, Leggio LL, Skriver K (2005) NAC transcription factors: Structurally distinct, functionally diverse. Trends Plant Sci **10:** 79–87

Pearce S, Ferguson A, King J, Wilson ZA (2015) FlowerNet: A gene expression correlation network for anther and pollen development. Plant Physiol **167:** 1717–1730

Persson S, Wei H, Milne J, Page GP, Somerville CR (2005) Identification of genes required for cellulose synthesis by regression analysis of public microarray data sets. Proc Natl Acad Sci USA **102:** 8633–8638

Ruzin SE (1999) Plant Microtechnique and Microscopy. Oxford University Press, New York.

Sanders PM, Bui AQ, Weterings K, McIntire KN, Hsu YC, Lee PY, Truong MT, Beals TP, Goldberg RB (1999) Anther developmental defects in *Arabidopsis thaliana* male-sterile mutants. Sex Plant Reprod **11:** 297–322

Sambrook J, Fritsch E, Maniatis T (1989) Molecular cloning: A laboratory manual, 2nd Edition. Cold Spring Harbour

Scott RJ, Spielman M, Dickinson HG (2004) Stamen structure and function. Plant Cell **16**(**Suppl**): S46–S60

Steiner-Lange S, Unte US, Eckstein L, Yang C, Wilson ZA, Schmelzer E, Dekker K, Saedler H (2003) Disruption of *Arabidopsis thaliana* MYB26 results in male sterility due to non-dehiscent anthers. Plant J **34:** 519–528

Stockert JC, Cañete M, Colman OD (1984) Histochemical mechanism for the orthochromatic staining and fluorescence reaction of lignified tissues. Cell Mol Biol **30:** 503–508

Taylor NG, Howells RM, Huttly AK, Vickers K, Turner SR (2003) Interactions among three distinct CesA proteins essential for cellulose synthesis. Proc Natl Acad Sci USA **100:** 1450–1455

Taylor-Teeples M, Lin L, de Lucas M, Turco G, Toal TW, Gaudinier A, Young NF, Trabucco GM, Veling MT, Lamothe R, et al (2015) An

Arabidopsis gene regulatory network for secondary cell wall synthesis. Nature **517:** 571–575

Thévenin J, Pollet B, Letarnec B, Saulnier L, Gissot L, Maia-Grondard A, Lapierre C, Jouanin L (2011) The simultaneous repression of CCR and CAD, two enzymes of the lignin biosynthetic pathway, results in sterility and dwarfism in *Arabidopsis thaliana*. Mol Plant **4:** 70–82

Wang H, Avci U, Nakashima J, Hahn MG, Chen F, Dixon RA (2010) Mutation of WRKY transcription factors initiates pith secondary wall formation and increases stem biomass in dicotyledonous plants. Proc Natl Acad Sci USA **107:** 22338–22343

Wang H, Mao Y, Yang J, He Y (2015) TCP24 modulates secondary cell wall thickening and anther endothecium development. Front Plant Sci **6:** 436

Wang H, Zhao Q, Chen F, Wang M, Dixon RA (2011) NAC domain function and transcriptional control of a secondary cell wall master switch. Plant J **68:** 1104–1114

Wilson ZA, Song J, Taylor B, Yang C (2011) The final split: The regulation of anther dehiscence. J Exp Bot **62:** 1633–1649

Yamaguchi M, Kubo M, Fukuda H, Demura T (2008) Vascular-related NAC-DOMAIN7 is involved in the differentiation of all types of xylem vessels in Arabidopsis roots and shoots. Plant J **55:** 652–664

Yamaguchi M, Mitsuda N, Ohtani M, Ohme-Takagi M, Kato K, Demura T (2011) VASCULAR-RELATED NAC-DOMAIN7 directly regulates the expression of a broad range of genes for xylem vessel formation. Plant J **66:** 579–590

Yang C, Xu Z, Song J, Conner K, Vizcay Barrena G, Wilson ZA (2007) Arabidopsis MYB26/MALE STERILE35 regulates secondary thickening in the endothecium and is essential for anther dehiscence. Plant Cell **19:** 534–548

Zhao Q, Nakashima J, Chen F, Yin Y, Fu C, Yun J, Shao H, Wang X, Wang ZY, Dixon RA (2013) Laccase is necessary and nonredundant with peroxidase for lignin polymerization during vascular development in Arabidopsis. Plant Cell **25:** 3976–3987

Zhong R, Demura T, Ye ZH (2006) SND1, a NAC domain transcription factor, is a key regulator of secondary wall synthesis in fibers of Arabidopsis. Plant Cell **18:** 3158–3170

Zhong R, Lee C, Ye ZH (2010) Global analysis of direct targets of secondary wall NAC master switches in Arabidopsis. Mol Plant **3:** 1087–1103

Zhong R, Lee C, Zhou J, McCarthy RL, Ye ZH (2008) A battery of transcription factors involved in the regulation of secondary cell wall biosynthesis in Arabidopsis. Plant Cell **20:** 2763–2782

Zhong R, Ye ZH (2014) Complexity of the transcriptional network controlling secondary wall biosynthesis. Plant Sci **229:** 193–207

Zhong R, Ye ZH (2015) The Arabidopsis NAC transcription factor NST2 functions together with SND1 and NST1 to regulate secondary wall biosynthesis in fibers of inflorescence stems. Plant Signal Behav **10:** e989746

Zhou J, Zhong R, Ye ZH (2014) Arabidopsis NAC domain proteins, VND1 to VND5, are transcriptional regulators of secondary wall biosynthesis in vessels. PLoS One **9:** e105726